Article

Cell

Eukaryotic Acquisition of a Bacterial Operon

Graphical Abstract

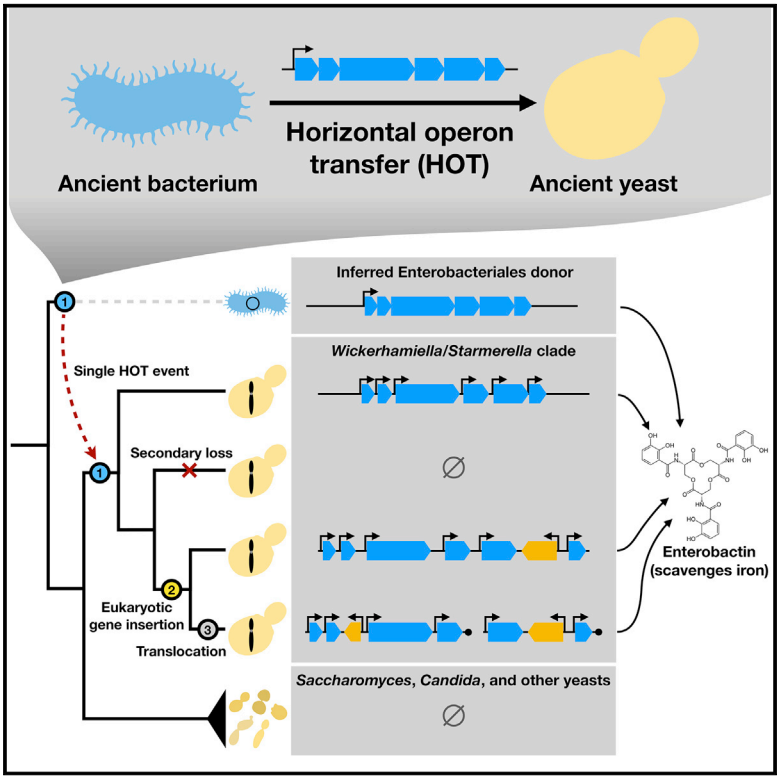

Authors

Jacek Kominek, Drew T. Doering, Dana A. Opulente, ..., Cletus P. Kurtzman, Antonis Rokas, Chris Todd Hittinger

Correspondence

cthittinger@wisc.edu

In Brief

Horizontal gene transfer of a full operon encoding siderophore biosynthesis genes from bacteria to a group of budding yeasts was followed by acquisition of eukaryotic genomic and transcriptional features.

Highlights

- Some yeast species harbor enterobactin biosynthesis genes unseen in other fungi
- An ancient horizontal operon transfer occurred from bacteria to a group of yeasts
- The operon underwent genetic changes after transfer to a eukaryotic genome
- The genes are expressed monocistronically and result in enterobactin production

Kominek et al., 2019, Cell *176*, 1356–1366
March 7, 2019 © 2019 Elsevier Inc.
https://doi.org/10.1016/j.cell.2019.01.034

CellPress

Cell

Article

Eukaryotic Acquisition of a Bacterial Operon

Jacek Kominek,[1,2,9] Drew T. Doering,[1,2,3,9] Dana A. Opulente,[1,2] Xing-Xing Shen,[4] Xiaofan Zhou,[4,5] Jeremy DeVirgilio,[6] Amanda B. Hulfachor,[1] Marizeth Groenewald,[7] Mcsean A. Mcgee,[2] Steven D. Karlen,[2,8] Cletus P. Kurtzman,[6,10] Antonis Rokas,[4] and Chris Todd Hittinger[1,2,3,11,*]

[1]Laboratory of Genetics, Genome Center of Wisconsin, Wisconsin Energy Institute, J.F. Crow Institute for the Study of Evolution, University of Wisconsin-Madison, Madison, WI 53706, USA
[2]DOE Great Lakes Bioenergy Research Center, University of Wisconsin-Madison, Madison, WI 53706, USA
[3]Graduate Program in Cellular and Molecular Biology, University of Wisconsin-Madison, Madison, WI 53706, USA
[4]Department of Biological Sciences, Vanderbilt University, Nashville, TN 37235, USA
[5]Guangdong Province Key Laboratory of Microbial Signals and Disease Control, Integrative Microbiology Research Centre, South China Agricultural University, 510642 Guangzhou, China
[6]Mycotoxin Prevention and Applied Microbiology Research Unit, National Center for Agricultural Utilization Research, Agricultural Research Service, US Department of Agriculture, Peoria, IL 61604, USA
[7]Westerdijk Fungal Biodiversity Institute, 3584 CT, Utrecht, Netherlands
[8]Department of Biochemistry, University of Wisconsin-Madison, Madison, WI 53706, USA
[9]These authors contributed equally
[10]Deceased
[11]Lead Contact
*Correspondence: cthittinger@wisc.edu
https://doi.org/10.1016/j.cell.2019.01.034

SUMMARY

Operons are a hallmark of bacterial genomes, where they allow concerted expression of functionally related genes as single polycistronic transcripts. They are rare in eukaryotes, where each gene usually drives expression of its own independent messenger RNAs. Here, we report the horizontal operon transfer of a siderophore biosynthesis pathway from relatives of *Escherichia coli* into a group of budding yeast taxa. We further show that the co-linearly arranged secondary metabolism genes are expressed, exhibit eukaryotic transcriptional features, and enable the sequestration and uptake of iron. After transfer, several genetic changes occurred during subsequent evolution, including the gain of new transcription start sites that were sometimes within protein-coding sequences, acquisition of polyadenylation sites, structural rearrangements, and integration of eukaryotic genes into the cluster. We conclude that the genes were likely acquired as a unit, modified for eukaryotic gene expression, and maintained by selection to adapt to the highly competitive, iron-limited environment.

INTRODUCTION

The core processes of the central dogma of biology, transcription and translation, are broadly conserved across living organisms. Nonetheless, there are seemingly fundamental differences between the domains of life in how these processes are realized. Eukaryotic transcription is spatially and temporally separated from translation and generally operates on individual genes through a complex interplay of transcription factors and chromatin remodeling complexes. Nascent mRNAs are co-transcriptionally processed by adding 3′ polyadenosine (poly(A)) tails and 5′ caps of 7-methyl-guanosine (m^7G) before they are trafficked out of the nucleus for translation. In bacteria, transcription is tightly coupled with translation, and both occur inside the cytosol. Furthermore, bacterial transcription often operates on clusters of genes, known as operons, where a single regulatory region controls the expression of physically linked genes into a polycistronic mRNA that is minimally processed and translated into several polypeptides at similar abundances. In contrast, eukaryotic operons, which are rare in most taxa but are frequently found in nematodes (Blumenthal and Gleason, 2003; Spieth et al., 1993) and tunicates (Ganot et al., 2004; Vandenberghe et al., 2001), are processed by *trans*-splicing and related mechanisms.

Operon dissemination has been proposed to occur predominantly via horizontal gene transfer (HGT) (Lawrence and Roth, 1996; Omelchenko et al., 2003), a process where organisms acquire genes from sources other than their parents. HGT is pervasive and richly documented among bacteria, but it is rarer in eukaryotes (Alexander et al., 2016; Keeling and Palmer, 2008; Richards et al., 2011a; Slot and Rokas, 2011; Soucy et al., 2015). Recently, several examples of horizontal gene transfer from archaea or bacteria into eukaryotes have been uncovered, and most of these have involved individual genes that are sometimes functionally related, such as genes involved in nucleic acid synthesis and salvage from bacteria into Microsporidia (Alexander et al., 2016), a gene of uncertain origin into Cnidarians (Dana et al., 2012), osmotrophy-related genes from fungi into oomycetes (Richards et al., 2006), various metabolic pathways assembled in several steps from multiple unassociated bacteria into mealybugs (Husnik et al., 2013; Husnik and McCutcheon, 2016), and several examples of bacterial genes into dikaryon fungi (Fitzpatrick, 2012; Marcet-Houben and Gabaldón, 2010).

Only a handful of known cross-domain transfer events have involved multiple genes in a single transfer event. Portions of the genome of an intracellular bacterial endosymbiont of insects have been found in insect genomes, with the transferred chunks ranging in size from roughly 500 bp to nearly the entire endosymbiont genome (Kondo et al., 2002; Nikoh et al., 2008; Dunning Hotopp et al., 2007). Furthermore, the plastid genomes of some eustigmatophyte algae harbor an operon of bacterial origin, although the function of the transferred genes in this case is uncertain (Yurchenko et al., 2016, 2018). A two-gene operon of archaeal origin was discovered in the protist *Pygsuia* nuclear genome, but these genes were subsequently fused into a single open reading frame (ORF) (Stairs et al., 2014). This fused two-gene operon can also be found in the nuclear genome of the anaerobic human protozoan parasite *Blastocystis* (Tsaousis et al., 2012). It is unclear whether this operon was first transferred to the *Pygsuia* or the *Blastocystis* lineage, but both are found in low-oxygen environments: *Pygsuia* from hypoxic marine sediments and *Blastocystis* from human gastrointestinal tracts. Additionally, three genes (two of which are now fused into a single ORF in some taxa) from the bacterial peptidoglycan biosynthesis operon can be found in extant *Aspergillus* spp., although their phylogenetic origin is not fully resolved (Marcet-Houben and Gabaldón, 2010). Despite these tantalizing examples, it remains unclear (1) whether eukaryotes can acquire new traits or capabilities via the horizontal transfer of operons encoding complex multi-gene pathways from free-living bacteria in a single event, (2) whether the expression of such an operon is compatible with the seemingly conflicting characteristics of transcription and translation in a eukaryotic nuclear genome, and (3) how the function of the operon can subsequently be maintained following integration into the eukaryotic genome. Horizontal operon transfer (HOT) events could allow even complex pathways to spread rapidly across domains of life, especially in environments where competition for key nutrients is intense.

One such nutrient is iron, which plays crucial roles in many essential cellular processes (Andrews et al., 2003; Sheftel et al., 2010; Sutak et al., 2008) and is a key determinant of virulence in both animal and plant pathogens (Scharf et al., 2014; Skaar 2010; Toth et al., 2006). Many specialized systems have evolved to sequester iron from the surrounding environment, one of which is the biosynthesis of small-molecule iron chelators called siderophores. Most bacteria synthesize catecholate-class siderophores (Wandersman and Delepelaire, 2004), whereas hydroxamate-class siderophores are commonplace in fungi (Haas et al., 2008). A notable exception is the budding yeast lineage (subphylum Saccharomycotina), which has long been thought to completely lack the ability to synthesize their own siderophores, despite its ability to utilize those produced by other microbes (Haas et al., 2008).

Here, we survey a broad range of fungal genomes for known components of iron uptake and storage systems. Although most systems are broadly conserved, we identify a clade of closely related yeast species that contains a bacterial siderophore biosynthesis pathway. Through phylogenetic hypothesis testing, we show that this pathway was acquired through horizontal operon transfer (HOT) from the bacterial order Enterobacteriales, which includes, among others, *Escherichia coli*, *Erwinia carotovora*, and *Yersinia pestis*. Relatives of those species share the insect gut niche with many yeasts of the recipient clade (Gilliam and Valentine, 1974; Gilliam 1997, Moran et al., 2008, Lachance et al., 2001; Rosa et al., 2003). After acquisition, the operon underwent structural changes and successively gained eukaryotic characteristics, while maintaining the clustering of functionally related genes. Transcriptomic experiments show that the transferred siderophore biosynthesis genes are actively expressed in a manner largely consistent with canonical eukaryotic transcription, and *in vivo* assays demonstrate that the operon is functional in most yeast species that contain it. This remarkable example shows how eukaryotes can acquire a functional bacterial operon, while modifying its transcription to domesticate and maintain expression as a set of linked eukaryotic genes.

RESULTS

Iron Uptake and Storage Is Conserved in Fungi

We surveyed the genome sequences of 175 dikaryon fungal species and observed broad conservation of genes involved in low-affinity iron uptake, vacuolar iron storage, reductive iron assimilation, and siderophore import systems (Figure 1; Table S1). In contrast, genes involved in siderophore biosynthesis pathways were more varied in terms of presence and type. Siderophore biosynthesis gene clusters were thought to be completely absent in budding yeasts (Haas et al., 2008), but the genomes of *Lipomyces starkeyi* and *Tortispora caseinolytica* contain homologs of the *SidA*, *SidC*, *SidD*, *SidF*, and *SidL* genes involved in the biosynthesis of ferricrocin and fusarinine C, which are hydroxamate-class siderophores synthesized from L-ornithine by many filamentous fungi, such as *Aspergillus nidulans* (Haas et al., 2008). Because these species are highly divergent from all other budding yeast taxa with sequenced genomes, the presence of this pathway in their genomes is likely an ancestral trait inherited from the last common ancestor of the Pezizomycotina and Saccharomycotina, while its absence in most yeasts is likely due to a loss early in budding yeast evolution. A handful of phylogenetically diverse set of budding yeast species contain the newly discovered gene cluster for synthesizing the siderophore pulcherrimin (Krause et al., 2018). Surprisingly, the genomes of three closely related Trichomonascaceae species (*Wickerhamiella* (*Candida*) *versatilis*, *Starmerella* (*Candida*) *apicola*, and *Starmerella bombicola*) contain multiple homologs of bacterial siderophore biosynthesis genes (*entA–entF*) that are predicted to enable the synthesis of catecholate-class siderophores from chorismate (Adeolu et al., 2016) (Figure S1). These genes are co-linear and predicted to be expressed from the same strand of DNA, features that are both reminiscent of the operons where these genes are found in bacteria.

Horizontal Operon Transfer from Bacteria to Yeasts

To investigate the evolutionary history of these genes, we sequenced and analyzed 17 additional genomes from the *Wickerhamiella*/*Starmerella* clade (W/S clade; Table S1) and identified the catecholate-class siderophore biosynthesis pathway in 12 of these species (Figures 2A and 2C). The genes were located on high-coverage contigs that contained multiple

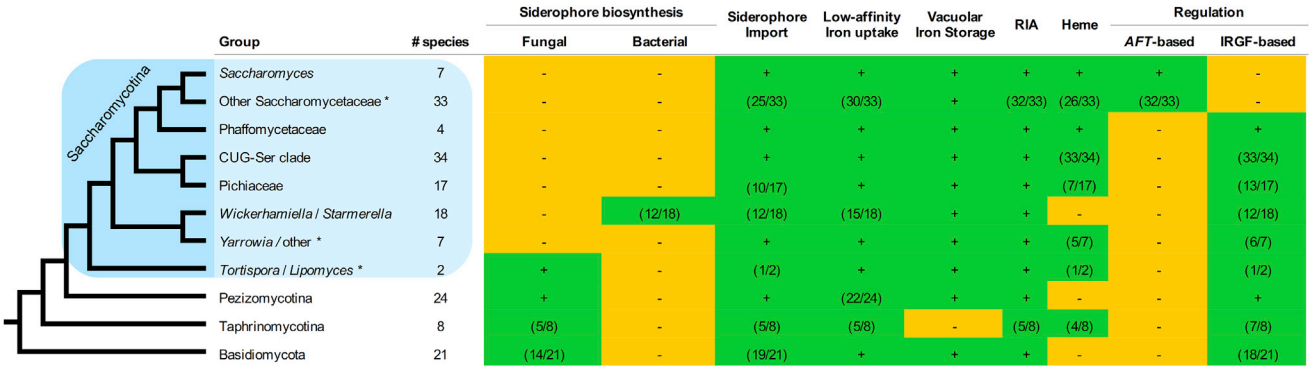

Group	# species	Siderophore biosynthesis: Fungal	Siderophore biosynthesis: Bacterial	Siderophore Import	Low-affinity Iron uptake	Vacuolar Iron Storage	RIA	Heme	Regulation: *AFT*-based	Regulation: IRGF-based
Saccharomyces	7	-	-	+	+	+	+	+	+	-
Other Saccharomycetaceae *	33	-	-	(25/33)	(30/33)	+	(32/33)	(26/33)	(32/33)	-
Phaffomycetaceae	4	-	-	+	+	+	+	+	-	+
CUG-Ser clade	34	-	-	+	+	+	+	(33/34)	-	(33/34)
Pichiaceae	17	-	-	(10/17)	+	+	+	(7/17)	-	(13/17)
Wickerhamiella / Starmerella	18	-	(12/18)	(12/18)	(15/18)	+	+	-	-	(12/18)
Yarrowia / other *	7	-	-	+	+	+	+	(5/7)	-	(6/7)
Tortispora / Lipomyces *	2	+	-	(1/2)	+	+	+	(1/2)	-	(1/2)
Pezizomycotina	24	+	-	+	(22/24)	+	+	-	-	+
Taphrinomycotina	8	(5/8)	-	(5/8)	(5/8)	-	(5/8)	(4/8)	-	(7/8)
Basidiomycota	21	(14/21)	-	(19/21)	+	+	+	-	-	(18/21)

Figure 1. Distribution of the Iron Uptake and Storage Systems among Fungi

Plus (green) and minus (orange) signs indicate the presence and absence of iron uptake and storage systems in specific taxonomic groups. The numbers in parentheses (green) indicate the number of species in a taxonomic group that possess a specific system, if it is not ubiquitous in that group. The blue box indicates the budding yeasts. RIA, reductive iron assimilation; IRGF, iron-responsive GATA factor. Asterisks mark paraphyletic groups. Note that only *Wickerhamiella/Starmerella* (W/S) clade fungi contain the bacterial or catecholate-class siderophore biosynthesis pathway, whereas many other dikaryon fungi contain hydroxamate-class siderophore biosynthesis pathways.

See also Figure S1 and Table S1.

other yeast genes, which assured us that they were not a product of contamination (Table S1). To determine whether the yeast siderophore biosynthesis genes were horizontally acquired from a bacterial operon, we first used the *ent*erobactin genes found in yeasts to perform BLAST queries against the bacterial data present in GenBank and found that the top hits belonged to a range of species from the order Enterobacteriales. Because no single taxon was overrepresented, we surveyed 1,336 publicly available genomes from the class Gammaproteobacteria, to which the order Enterobacteriales belongs, for the presence of *entA-entF* homologs and extracted them from all 207 genomes where all six genes could be reliably identified (Table S2). We then reconstructed unconstrained maximum-likelihood (ML) phylogenies for each *ent* gene, as well as for a concatenated super-alignment of all six genes (*entABCDEF*) (Table S2). Because *entF* contributed nearly two-thirds of the total alignment length, we also evaluated a super-alignment of the remaining five genes (*entABCDE*) (Figure 2A).

Consistent with the BLAST results, the yeast sequences formed a highly supported, monophyletic group nested within the Enterobacteriales lineage. The *ent* gene phylogenies of the Enterobacteriales were largely congruent with accepted relationships within the order (Adeolu et al., 2016; Baumler et al., 2013), and they placed the *ent* donor lineage as diverging from its common ancestor with *E. coli* after its divergence from *Serratia* and several other genera, but before the divergence of the *Pantoea/Erwinia* clade and *E. coli*. To formally test the hypothesis of an Enterobacteriales origin, we reconstructed phylogenies under the constraints that yeast sequences either grouped together with the Enterobacteriales (EO) or outside of that clade (non-EO). We then employed the approximately unbiased (AU) tests to determine if the EO phylogenies were a statistically better explanation of the data than the non-EO phylogenies. The EO phylogeny was strongly preferred (p value $< 10^{-3}$) for the six- and five-gene concatenation data matrices (Figure 2D). Individual genes carried weak signal due to their short lengths, but the *entC*, *entE*, and *entF* genes nonetheless supported the Enterobacteriales origin (p value < 0.05); *entA* and *entB* had consistent but weaker support; and no individual gene rejected the EO hypothesis. Next, we sought to determine the course of the transfer event and tested a single-source, single-transfer hypothesis against multi-source and multi-transfer alternatives, each of which predicted specific phylogenetic patterns (Figure 2C). AU tests on the reconstructed phylogenies did not support multiple transfer events and, instead, supported the simplest explanation that the horizontal operon transfer (HOT) event occurred from a single source lineage directly into a single common ancestor of the W/S clade yeasts (Figure 2D).

The Bacterial Siderophore Biosynthesis Pathway Is Functional in Yeasts

To determine whether yeasts that contain the *ent* biosynthesis genes actually produce siderophores, we grew them on a low-iron medium overlaid with an agarose solution containing iron-complexed chromeazurol S (CAS), a colorimetric indicator of iron chelation. In presence of iron chelators, such as siderophores, the indicator changes color from blue to orange in a characteristic halo pattern that tracks the diffusion gradient of siderophores secreted from colonies into the surrounding medium. We tested the 18 yeast species from the W/S clade, together with eight outgroup species spread broadly across the yeast phylogeny (including *S. cerevisiae*), and *E. coli* as a positive control. We observed strong signals of siderophore production in six yeast species, all of which contain the siderophore biosynthesis genes (Figures 3B and S4). The lack of signal in other species harboring the siderophore biosynthesis genes could suggest that siderophore production was below the sensitivity of the O-CAS assay under the conditions studied. Conversely, the O-CAS assay could lead to false positives if other mechanisms were sufficiently capable of sequestering iron. Thus, we used high-performance liquid chromatography with tandem mass spectrometry (HPLC-MS/MS) to specifically

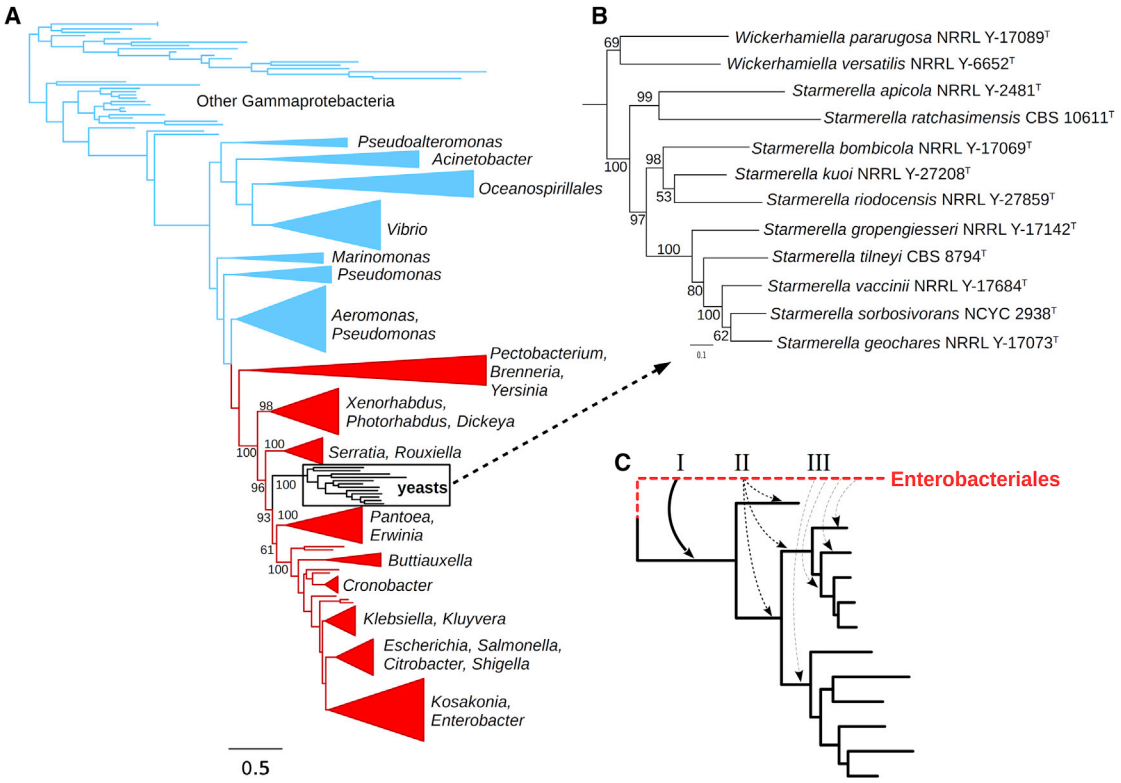

D

	Question	Was the source from Enterobacteriales (EO)?	Was there a single source of genes? (I & II vs III)	Was there a single transfer event? (I vs II)
	Topologies tested	EO vs non-EO origin	12-mono vs 11-mono	ML / 5G
Genes	***entA***	0.9121 / 0.0879	0.5735 / 0.3751	0.8804 / 0.1196
	entB	0.8706 / 0.1294	0.4563 / 0.2801	0.6752 / 0.3248
	entC	0.9869 / 0.0131	0.4397 / 0.4318	0.7543 / 0.2457
	entD	0.1452 / 0.8423	0.5152 / 0.2809	0.7495 / 0.2505
	entE	0.9842 / 0.0158	0.4751 / 0.3884	0.8326 / 0.1674
	entF	0.9996 / 0.0004	0.551 / 0.335	0.8946 / 0.1054
	ABCDE	0.9995 / 0.0005	0.4519 / 0.4292	-
	ABCDEF	1.0000 / 0.0000	0.5897 / 0.23	0.8355 / 0.1645
	Result	Non-EO topology rejected	Monophyly supported	Consistent topology supported
	Conclusion	Enterobacteriales origin	Single source of genes	Single transfer event

Figure 2. Yeast Siderophore Biosynthesis Originated from an Enterobacteriales Lineage

(A) ML phylogeny from the super-alignment of *entABCDE* genes from 207 Gammaproteobacteria and 12 yeasts, rooted at the midpoint. Bootstrap support values are shown for relevant branches within the Enterobacteriales (red). Other Gammaproteobacteria are blue.

(B) Detailed view of the yeast clade from the main phylogeny with bootstrap support values.

(C) Alternative scenarios for the horizontal operon transfer.

(D) p values of the AU tests of different evolutionary hypotheses. EO, Enterobacteriales origin; non-EO, non-Enterobacteriales origin; 12-mono, 12 yeast sequences are monophyletic, 11-mono, 11 yeast sequences monophyletic and one unconstrained (12 alternatives tested, lowest p value shown, full details in Table S2); 5G, topology of the yeast clade constrained to the one inferred from the super-alignment of *entABCDE* genes. Shimodaira-Hasegawa (SH) tests had less statistical power but produced fully concordant results.

See also Tables S1 and S2.

detect the chemical enterobactin. Under our strict thresholds for detection across multiple experiments and conditions, 9/12 yeast species harboring the siderophore biosynthesis genes were scored as enterobactin producers (Figure 3B). Taken together, these experiments conclusively show that the bacterial siderophore biosynthesis genes are fully functional in at least some W/S clade yeasts.

Evolution of a Bacterial Operon inside a Eukaryotic Host

Given the significant differences in central dogma processes between bacteria and eukaryotes, we investigated how the horizontally transferred operon was successfully assimilated into these yeasts. The lengths of intergenic regions were not divisible by three, so we immediately excluded the hypothesis that they were translated as a single fused polypeptide that could be

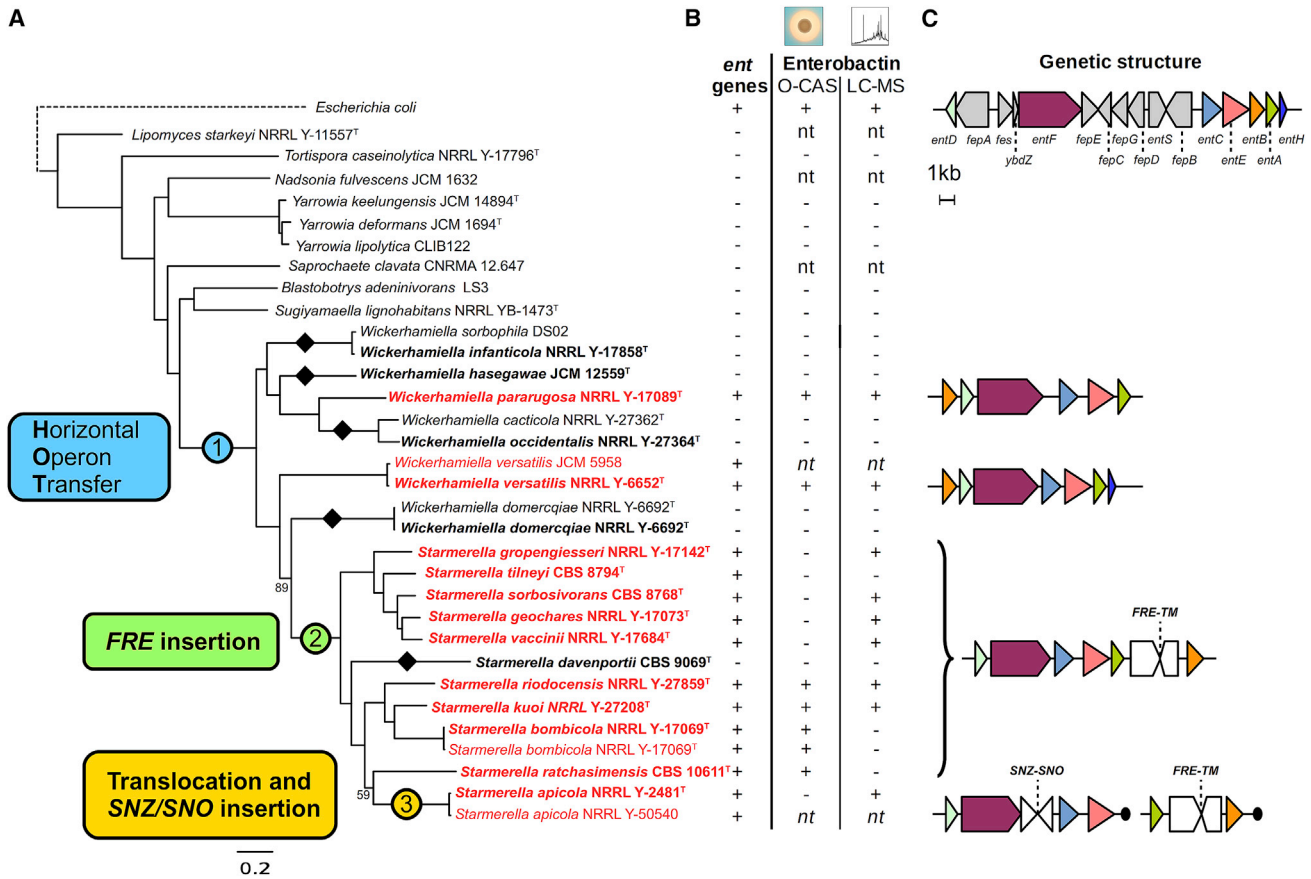

Figure 3. Evolution of the Siderophore Biosynthesis Genes in Yeasts

(A) ML phylogeny reconstructed from the concatenated alignment of 661 conserved, single copy genes (834,750 sites), with branch support values below 100 shown. Strains in bold denote genomes sequenced in this study, while strains in red denote genomes containing the siderophore biosynthesis genes. Black diamonds indicate secondary losses in yeast lineages, accompanied by losses of the siderophore importer *ARN* genes, which are often found in close proximity. (1) Horizontal operon transfer from an Enterobacteriales lineage. (2) Rearrangement and integration of genes encoding ferric reductase (*FRE*) and an uncharacterized transmembrane protein (*TM*). (3) Disruption by integration of the *SNZ-SNO* gene pair and translocation.

(B) Species-specific data on presence or absence of the siderophore biosynthesis genes and experimental evidence for the presence of enterobactin in the yeast cultures as determined by an O-CAS assay (not specific to enterobactin) and direct chemical detection by HPLC-MS/MS (enterobactin produced by *E. coli* was used as the standard; nt, not tested). Note that culture conditions between assays were not identical, and siderophore expression is often condition-dependent (Machuca and Milagres, 2003).

(C) Genetic structure of the siderophore biosynthesis operon in *E. coli* and yeasts, drawn to scale. Individual colors represent homologous genes, and gray marks represent bacterial genes not found in yeasts. Black circles represent contig termini within 25 kb.

See also Figure S4 and Table S4.

produced from a single transcript by stop codon read-through. Next, we mapped several key changes in gene content, structure, and regulation onto the yeast phylogeny (Figure 3). First, the phylogenetic distribution of the operon genes suggests at least five cases of secondary loss in W/S clade yeasts, a common evolutionary mode for other fungal gene clusters (Campbell et al., 2013; Khaldi et al., 2008; Proctor et al., 2013; Slot and Rokas, 2010). Although all taxa contain the six core genes (*entA-F*), *W. versatilis* uniquely harbors a homolog of the *entH* gene, which encodes a proofreading thioesterase that is not strictly required for siderophore biosynthesis (Leduc et al., 2007). Because no homologs or remnants of other genes from the bacterial operon could be identified, we hypothesize that they were lost due to functional redundancy with genes already present in yeast genomes (e.g., the bacterial ABC transporter genes *fepA–fepG* are functionally similar to the yeast major facilitator superfamily transporter genes *ARN1–ARN4*, while the bacterial esterase gene *fes* is functionally similar to yeast ferric reductase genes *FRE1–FRE8*). Second, most extant Enterobacteriales species closely related to the source lineage share an operon structure similar to that of *E. coli* (Table S2), which is more complex than that of the W/S clade yeasts (Figure 3C). Based on the high amount of sequence divergence, we infer that an ancient bacterial operon, whose structure was somewhere between that of *E. coli* and *W. versatilis*, was horizontally transferred into a yeast cell tens of millions of years ago. The operon may have contained fewer genes than extant bacterial operons, or shared gene losses or rearrangements may have occurred to produce a

structure similar to that of *W. versatilis* in the last common ancestor of the W/S clade yeasts. Third, modern yeasts of this clade have evolved at least four different structures through several lineage-specific rearrangements that tended to create derived gene cluster structures with more eukaryotic characteristics, including increasing the size of the intergenic regions, splitting the gene cluster in two in *St. apicola*, and intercalating at least four eukaryotic genes. The intercalation of a gene encoding a eukaryotic ferric reductase (*FRE*), which is involved in reductive iron assimilation, between two operon genes in a subset of species offers a particularly telling example. The genetic linkage of these two mechanisms for acquiring iron shows that bacterial and eukaryotic genes can stably co-exist and perhaps even be selected together as gene clusters for co-inheritance or co-regulation, through eukaryotic mechanisms.

Transferred Genes Have Mainly Eukaryotic Transcript Features

To determine whether and how these yeasts overcame the differences between eukaryotic and bacterial gene expression, we used a strand-specific protocol to sequence mRNA from *W. versatilis*, *St. apicola*, and *St. bombicola*. These species were chosen due to their diverse gene cluster structures and positions on the phylogenetic tree: *W. versatilis* was chosen because its structure was likely more similar to the ancestral operon, while *St. bombicola* and *St. apicola* appeared to represent more derived stages of evolution in the eukaryotic hosts. Each of the three species expressed mRNAs for the siderophore biosynthesis genes, and *W. versatilis* expression was the highest (Table S3). The *W. versatilis* genes were expressed at similar levels, whereas *St. bombicola* and *St. apicola* genes showed significant diversity in their expression (Figures 4, S2, S3, and S4; Table S3). Interestingly, we also observed that the siderophore biosynthesis genes in *W. versatilis* had much shorter intergenic sequences than their counterparts in *St. bombicola* and *St. apicola*, which were each shorter than their respective genome-wide means (within gene cluster means between predicted protein-coding sequences were 158, 484, and 377 bps versus genome-wide means of 370, 549, and 455 bps for *W. versatilis*, *St. bombicola*, and *St. apicola*, respectively).

To further investigate operon-like characteristics that may have been retained, we searched our RNA sequencing (RNA-seq) data for read-pairs in which each paired read mapped to a different predicted protein-coding sequences. Because both reads of a read-pair originate from the same mRNA molecule, crossmapping of read-pairs could suggest the presence of multiple protein-coding genes on the same transcript. In all three species, most transcripts predicted to be involved in siderophore biosynthesis were clearly monocistronic and included poly(A) tails, as expected from eukaryotic-style gene expression (Figures 4, S2, S3, and S4). We did not find any evidence suggesting that 5′ caps were added by *trans*-splicing (Van Doren and Hirsh, 1990) or by alternatively *cis*-splicing a common cassette exon upstream of each protein-coding region (Keren et al., 2010), common eukaryotic transcriptional processing mechanisms that could have produced monocistronic transcripts. Interestingly, *W. versatilis* produced substantial crossmapping reads for two gene pairs: *entB-entD* (232 bps apart) and *entA-entH* (22 bps apart) (Figure 4D). Previously reported yeast bicistronic transcripts have been attributed mainly to inefficiencies in the RNA transcription machinery (David et al., 2006; Pelechano et al., 2013), but given that the yeast *ent* transcripts encode functionally related steps of a single biosynthesis pathway originally encoded in a bacterial operon, we wondered whether they could have retained some polycistronic characteristics from their ancestry.

To test whether bicistronic transcripts of the siderophore biosynthesis genes were prevalent in *W. versatilis*, we used the RACE (rapid amplification of cDNA ends) approach to sequence the 5′ and 3′ ends of mRNAs of *W. versatilis* genes from the two pairs that showed the strongest signal of crossmapping reads (Figure 4E). For the *entB-entD* gene pair, we found evidence of several overlapping mRNAs (i.e., multiple distinct 3′ ends of mRNAs containing the *entB* gene overlapped with multiple distinct 5′ ends of mRNAs containing the *entD* gene), but we did not detect any evidence of bicistronic *entB-entD* mRNAs. In the case of the *entA-entH* gene pair, all detected 5′ ends of *entH* mRNAs overlapped substantially with the detected 3′ ends of *entA* mRNAs. Several of the 3′ ends of *entA* mRNAs were also downstream of the predicted *entH* protein-coding sequence. Although these observations are consistent with the presence of some level of bicistronic *entA-entH* transcripts, they do not strictly require this interpretation. Indeed, several of the detected 5′ transcription start sites for *entH* (by both RACE and a large spike in RNA-seq coverage) occurred within the protein-coding sequence of *entA*, and we never detected a 5′ transcription start site for *entH* upstream of *entA* by RACE. Because both the *entA* and *entH* genes express high levels of mRNAs where their own predicted translation start site would be the first one encountered downstream of their respective 5′ cap, the translation of multiple polypeptides from a single transcript is not required to explain the expression of either gene.

Thus, we conclude that, even in *W. versatilis*, the majority of these transcripts are transcribed and processed through conventional eukaryotic mechanisms that involve distinct promoters and polyadenylation sites for each gene. This densely packed locus produces mRNAs of considerable diversity, including overlapping transcripts, alternative transcription start and polyadenylation sites, transcription start sites within upstream protein-coding sequences, and anti-sense transcripts (Table S3). These observed transcriptional mechanisms suggest that the complexity and noisiness of eukaryotic transcription may have been key to allowing some amount of each gene product to have been expressed by the initially transferred operon.

DISCUSSION

The horizontal transfer of this siderophore biosynthesis operon has provided an exceptionally illuminating and clearly documented case of the acquisition of a complete multi-gene bacterial operon encoding a complex metabolic pathway by a eukaryotic nuclear genome in a single transfer event. Here, we have used phylogenetic hypothesis testing to demonstrate that the *ent* operon was transferred from the Enterobacteriales lineage into an ancestor of the W/S clade of yeasts in a single event. As the lineage diversified, the operon subsequently underwent

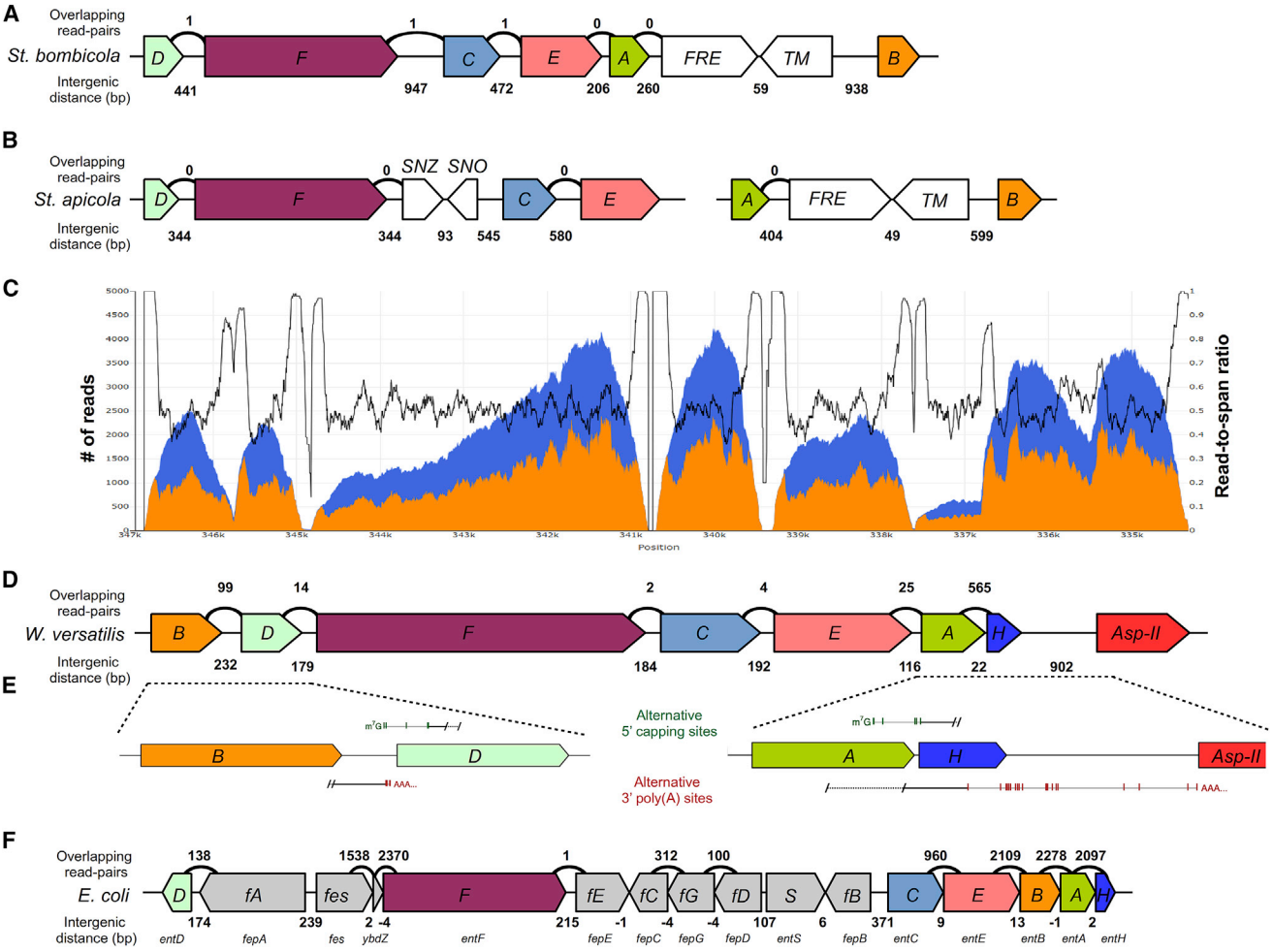

Figure 4. Transcriptomics of the Siderophore Biosynthesis Genes in *W. versatilis*

(A, B, and D) Diagram of siderophore biosynthesis genes as present in the genomes of *St. bombicola* (A), *St. apicola* (B), and *W. versatilis* (D), drawn to scale. Counts above the diagram indicate read-pairs that map to both predicted protein-coding sequences (low, non-zero read counts are likely DNA contamination). Counts below indicate the size of intergenic regions between adjacent protein-coding sequences, in base pairs.

(C) The orange area indicates per-base coverage by RNA-seq reads (read coverage). The blue area indicates per-base cumulative coverage by RNA-seq reads and inserts between read-pairs (span coverage). The black line indicates the ratio of the read coverage over the span coverage, which is expected to remain ~50% in the middle of gene transcripts and rise toward 100% at transcript termini. Thus, transcript boundaries are visualized as a coverage trough between two spikes that approach 100% ratios. Ratios below 100% at the putative 5′ or 3′ ends of annotated transcripts, coupled with non-zero coverage of their intergenic regions, suggest overlapping or potentially bicistronic transcripts. The expected 3′ coverage bias can be observed for individual transcripts in the raw coverage data.

(E) Results of 5′ and 3′ RACE experiments, depicting the positions of all detected m^7G caps (green vertical lines) and poly(A) tails (red vertical lines) in the *entB-entD* (left) and *entA-entH* (right) gene pairs in *W. versatilis.* The outer and inner gene-specific primers are marked by diagonal black lines and were used along with outer and inner primers specific to the 5′ or 3′ RACE adapters provided in the kit (see STAR Methods), which were adjacent to either the 5′ m^7G cap or the 3′ poly(A) tail, respectively. Dotted lines indicate sequences amplified only during the outer nested RACE PCR step, while solid lines indicate the portions of the transcripts that were amplified during the inner nested RACE PCR step and that were subsequently cloned for sequencing.

(F) Diagram of siderophore biosynthesis genes as present in the *E. coli* genome drawn to scale. Counts above the diagram indicate read-pairs crossmapping between genes (based on data from Seo et al., 2014; complete coverage maps shown in Figure S3). Counts below indicate the size of intergenic regions between adjacent protein-coding sequences, in base pairs (negative numbers indicate overlap). The *f* prefix (*fA-fG*) indicates the *fepA-fepG* genes.

See also Figures S2 and S3 and Table S3.

structural changes in the recipient eukaryotic genome, including increased intergenic spacing, insertion of eukaryotic genes, separation onto separate contigs, and even outright loss in some cases. We use transcriptomics and RACE to demonstrate that the operon genes are expressed in a manner consistent with canonical eukaryotic transcription, namely that transcripts contain poly(A) tails and are mainly monocistronic. Interestingly, in some cases, the genes evolved new eukaryotic promoters driving the expression of overlapping transcripts. Finally, we used the O-CAS assay, coupled with HPLC-MS/MS, to demonstrate that most species harboring the operon do indeed produce enterobactin, confirming that the operon is fully functional.

The previous scarcity of evidence for HOT into eukaryotes led authors to propose barriers due to pathway complexity (Husnik and McCutcheon, 2018; Wisecaver and Rokas, 2015; Wisecaver et al., 2016) and differences in core central dogma processes (Keeling and Palmer, 2008; Richards et al., 2011b). Where could the transfer of the siderophore biosynthesis operon between Enterobacteriales and yeasts have occurred, and how could the bacterial operon have been functionally maintained in the yeasts' genomes? Eukaryotes have been proposed to acquire bacterial genes through several mechanisms, including virus-aided transmission (Routh et al., 2012), environmental stress-induced DNA damage and repair (Flot et al., 2013; Gladyshev et al., 2008), and a phagocytosis-based gene ratchet (Doolittle 1998). The yeast species that harbor the siderophore biosynthesis operon have been isolated predominantly from insects (Lachance et al., 2001; Rosa and Lachance, 1998; Rosa et al., 2003), where stable bacterial and eukaryotic communities coexist inside their guts (Gilliam 1997). Moreover, this niche harbors diverse Enterobacteriales populations in which horizontal gene transfer has been reported (Watanabe and Sato, 1998; Watanabe et al., 1998), and insect guts have recently been described as a "mating nest" for yeasts (Stefanini et al., 2016). Because Enterobacteriales and yeasts can conjugate directly in some cases (Heinemann and Sprague, 1989), and the size of the genomic segment encoding the *ent* operon in Enterobacteriales (16 kb) is within the range of other horizontal transfers reported in the literature, we propose that the last common ancestor of the W/S clade yeasts may have incorporated the operon from a bacterial co-inhabitant of an insect gut. Due to the intense competition for nutrients in this ecosystem, including a constant arms race with the host organism itself (Barber and Elde, 2015), yeasts capable of making their own siderophores and sequestering iron may have had a substantial advantage over those relying on siderophores produced by others. Whether due to ecological or molecular mechanisms, the W/S clade may be particularly prone to HGT because this clade was recently reported to have acquired multiple unlinked bacterial genes (Gonçalves et al., 2018), more than any other clade of known budding yeasts (Shen et al., 2018). Unlike some other HGT reports, the genes transferred into the W/S yeasts did not fuse into multi-domain proteins (Marcet-Houben and Gabaldón, 2010, Stairs et al., 2014, Tsaousis et al., 2012) nor did they gain any introns (Da Lage et al., 2013; Marcet-Houben and Gabaldón, 2010; Tsaousis et al., 2012). Because the donor bacterium lacked introns and budding yeasts are known to be depauperate of introns (Neuvéglise et al., 2011; Hooks et al., 2014; Dujon and Louis, 2017), there seems to have been little evolutionary pressure or insufficient genetic drift to acquire them post-transfer.

Given the fundamental differences between bacterial and eukaryotic gene regulation, how could a bacterial operon have been maintained in a eukaryotic genome upon transfer? If it had not been actively expressed and functional, the genes of the operon would have been rapidly lost from the genome through neutral evolutionary processes. Although eukaryotes do not encode proteins with significant similarity to the negative regulator Fur that controls the expression of the bacterial *ent* genes, their iron response is similarly governed by transcription factors that also belong to the GATA family, such as Fep1 in *S. pombe*, SreA in *A. nidulans*, or Sfu1 in *C. albicans*. Indeed, the consensus Fur-binding site (5′-*GATAAT*-3′) is remarkably similar to that of the fungal iron-responsive GATA factors (IRGFs, 5′-*WGATAA*-3′) (Chen et al., 2007; Haas et al., 2008). This similarity suggests the intriguing possibility that the siderophore genes could have readily switched from being regulated by a bacterial transcription factor to a eukaryotic transcription factor, at least for the most 5′ promoter. While not a necessary element for successful expression of the *ent* genes (because both Fur and IRGFs are negative regulators), it could have allowed expression of the transferred genes to be environmentally responsive upon transfer. In addition to containing an enrichment of DNA sequence motifs similar to IRGF binding sites, sequences upstream of the *ent* genes contain other enriched motifs that could be bound by transcriptional activators (Table S3). Determining whether any of these motifs or any other binding sites regulate the expression of the *ent* genes in W/S clade yeasts will require more detailed dissection.

Siderophores are highly potent chelators that can efficiently sequester iron at very low concentrations (Boukhalfa and Crumbliss, 2002), so even a low basal expression level of the newly acquired genes, such as from cryptic promoters within upstream protein-coding sequences, could have been enough to convey a considerable selective advantage. This initial eukaryotic expression, perhaps aided by inherently noisy transcriptional and translation processes that include leaky scanning and internal ribosome entry sites (IRESs), could then have been optimized by acquiring more eukaryotic characteristics, such as longer intergenic regions that were gradually refined into improved promoters, distinct polyadenylation sites, and a shift from polycistronic or overlapping transcripts to mainly monocistronic and non-overlapping transcripts. The incorporation of a eukaryotic gene encoding a ferric reductase would have further improved the efficiency of iron acquisition in the highly competitive ecological niche of insect guts, while enhancing the eukaryotic characteristics of the gene cluster. Our HOT finding dramatically expands the boundaries of cross-domain gene flow. The transfer, maintenance, expression, and adaptation of a multi-gene bacterial operon to a eukaryotic host underscore the flexibility of eukaryotic transcriptional and translational systems to produce adaptive changes from novel and unexpected sources of genetic information.

STAR★METHODS

Detailed methods are provided in the online version of this paper and include the following:

- KEY RESOURCES TABLE
- CONTACT FOR REAGENT AND RESOURCE SHARING
- EXPERIMENTAL MODEL AND SUBJECT DETAILS
- METHOD DETAILS
  - Genome sequencing
  - RNA sequencing
  - Mapping transcript ends by 3′ and 5′ RLM-RACE
  - Cloning and confirmation of RACE products
  - Microbial culturing and O-CAS assays
  - HPLC analysis of yeast culture extracts

- QUANTIFICATION AND STATISTICAL ANALYSIS
  - Identification of iron metabolism genes
  - Genome assembly and annotation
  - Phylogenetic reconstruction and tests
  - RNA-Seq analysis
  - Identification of enriched motifs in promoters
  - HPLC analysis of yeast culture extracts
- DATA AND SOFTWARE AVAILABILITY

SUPPLEMENTAL INFORMATION

Supplemental Information includes four figures and four tables and can be found with this article online at https://doi.org/10.1016/j.cell.2019.01.034.

ACKNOWLEDGMENTS

We thank David J. Eide and Michael D. Bucci for advice on low-iron media, Nicole T. Perna and Jeremy D. Glasner for *E. coli* strain MG1655, Michael G. Thomas, John Ralph, and the Eide, Perna, Rokas, and Hittinger labs for comments and discussions, RIKEN for publicly releasing 20 genome sequences prior to publication, Lucigen Corporation (Middleton, WI) for use of their Covaris for gDNA sonication, and the University of Wisconsin Biotechnology Center DNA Sequencing Facility for providing Illumina sequencing facilities and services. This work was conducted in part using the resources of the Wisconsin Energy Institute, the Center for High-Throughput Computing at the University of Wisconsin-Madison, and the UW Biotechnology Center DNA Sequencing Facility. This material is based upon work supported by the National Science Foundation (DEB-1442113 to A.R. and DEB-1442148 to C.T.H. and C.P.K.), in part by the DOE Great Lakes Bioenergy Research Center (DOE BER Office of Science DE-SC0018409 and DE-FC02-07ER64494 to Timothy J. Donohue, director), the USDA National Institute of Food and Agriculture (Hatch Project 1003258 to C.T.H.), NIH (NIAID AI105619 to A.R.), and a Guggenheim Fellowship (to A.R). C.T.H. is a Pew Scholar in the Biomedical Sciences and a Vilas Early Career Investigator, supported by the Pew Charitable Trusts and Vilas Trust Estate, respectively. D.T.D. was supported by a NHGRI training grant to the Genomic Sciences Training Program (5T32HG002760). Mention of trade names or commercial products in this publication is solely for the purpose of providing specific information and does not imply recommendation or endorsement by the U.S. Department of Agriculture (USDA). The USDA is an equal opportunity provider and employer.

AUTHOR CONTRIBUTIONS

J.K. (study design, genome assembly, annotation, phylogenetic analyses, RNA-seq data analysis, text); D.T.D. (study design, O-CAS assays, RNA isolation and strand-specific library preparation, RACE experiments, LC-MS sample preparation, text); D.A.O., J.D.V., and A.B.H. (genomic DNA isolation and library preparation); X.-X.S. and X.Z. (preliminary genomic analyses); M.A.M. and S.D.K. (LC-MS experiments and analysis); M.G. and C.P.K. (strains); and C.P.K., A.R., and C.T.H. (study design, text).

DECLARATION OF INTERESTS

The authors declare no competing interests.

Received: October 31, 2018
Revised: December 20, 2018
Accepted: January 23, 2019
Published: February 21, 2019

REFERENCES

Adeolu, M., Alnajar, S., Naushad, S., and S Gupta, R. (2016). Genome-based phylogeny and taxonomy of the '*Enterobacteriales*': proposal for *Enterobacterales* ord. nov. divided into the families *Enterobacteriaceae, Erwiniaceae* fam. nov., *Pectobacteriaceae* fam. nov., *Yersiniaceae* fam. nov., *Hafniaceae* fam. nov., *Morganellaceae* fam. nov., and *Budviciaceae* fam. nov. Int. J. Syst. Evol. Microbiol. *66*, 5575–5599.

Alexander, W.G., Wisecaver, J.H., Rokas, A., and Hittinger, C.T. (2016). Horizontally acquired genes in early-diverging pathogenic fungi enable the use of host nucleosides and nucleotides. Proc. Natl. Acad. Sci. USA *113*, 4116–4121.

Altschul, S.F., Gish, W., Miller, W., Myers, E.W., and Lipman, D.J. (1990). Basic local alignment search tool. J. Mol. Biol. *215*, 403–410.

Andrews, S.C., Robinson, A.K., and Rodríguez-Quiñones, F. (2003). Bacterial iron homeostasis. FEMS Microbiol. Rev. *27*, 215–237.

Bailey, T.L., Boden, M., Buske, F.A., Frith, M., Grant, C.E., Clementi, L., Ren, J., Li, W.W., and Noble, W.S. (2009). MEME SUITE: tools for motif discovery and searching. Nucleic Acids Res. *37* (suppl2), W202–W208.

Barber, M.F., and Elde, N.C. (2015). Buried treasure: evolutionary perspectives on microbial iron piracy. Trends Genet. *31*, 627–636.

Baumler, D.J., Ma, B., Reed, J.L., and Perna, N.T. (2013). Inferring ancient metabolism using ancestral core metabolic models of enterobacteria. BMC Syst. Biol. *7*, 46.

Blattner, F.R., Plunkett, G., 3rd, Bloch, C.A., Perna, N.T., Burland, V., Riley, M., Collado-Vides, J., Glasner, J.D., Rode, C.K., Mayhew, G.F., et al. (1997). The complete genome sequence of Escherichia coli K-12. Science *277*, 1453–1462.

Blumenthal, T., and Gleason, K.S. (2003). *Caenorhabditis elegans* operons: form and function. Nat. Rev. Genet. *4*, 112–120.

Boukhalfa, H., and Crumbliss, A.L. (2002). Chemical aspects of siderophore mediated iron transport. Biometals *15*, 325–339.

Campbell, M.A., Staats, M., van Kan, J.A.L., Rokas, A., and Slot, J.C. (2013). Repeated loss of an anciently horizontally transferred gene cluster in *Botrytis*. Mycologia *105*, 1126–1134.

Chen, Z., Lewis, K.A., Shultzaberger, R.K., Lyakhov, I.G., Zheng, M., Doan, B., Storz, G., and Schneider, T.D. (2007). Discovery of Fur binding site clusters in *Escherichia coli* by information theory models. Nucleic Acids Res. *35*, 6762–6777.

Chomczynski, P., and Sacchi, N. (1987). Single-step method of RNA isolation by acid guanidinium thiocyanate-phenol-chloroform extraction. Anal. Biochem. *162*, 156–159.

Da Lage, J.L., Binder, M., Hua-Van, A., Janeček, S., and Casane, D. (2013). Gene make-up: rapid and massive intron gains after horizontal transfer of a bacterial α-amylase gene to Basidiomycetes. BMC Evol. Biol. *13*, 40.

Dana, C.E., Glauber, K.M., Chan, T.A., Bridge, D.M., and Steele, R.E. (2012). Incorporation of a horizontally transferred gene into an operon during cnidarian evolution. PLoS ONE *7*, e31643.

David, L., Huber, W., Granovskaia, M., Toedling, J., Palm, C.J., Bofkin, L., Jones, T., Davis, R.W., and Steinmetz, L.M. (2006). A high-resolution map of transcription in the yeast genome. Proc. Natl. Acad. Sci. USA *103*, 5320–5325.

Doolittle, W.F. (1998). You are what you eat: a gene transfer ratchet could account for bacterial genes in eukaryotic nuclear genomes. Trends Genet. *14*, 307–311.

Dujon, B.A., and Louis, E.J. (2017). Genome diversity and evolution in the budding yeasts (Saccharomycotina). Genetics *206*, 717–750.

Dunning Hotopp, J.C., Clark, M.E., Oliveira, D.C.S.G., Foster, J.M., Fischer, P., Muñoz Torres, M.C., Giebel, J.D., Kumar, N., Ishmael, N., Wang, S., et al. (2007). Widespread lateral gene transfer from intracellular bacteria to multicellular eukaryotes. Science *317*, 1753–1756.

Fitzpatrick, D.A. (2012). Horizontal gene transfer in fungi. FEMS Microbiol. Lett. *329*, 1–8.

Flot, J.F., Hespeels, B., Li, X., Noel, B., Arkhipova, I., Danchin, E.G.J., Hejnol, A., Henrissat, B., Koszul, R., Aury, J.M., et al. (2013). Genomic evidence for ameiotic evolution in the bdelloid rotifer *Adineta vaga*. Nature *500*, 453–457.

Ganot, P., Kallesøe, T., Reinhardt, R., Chourrout, D., and Thompson, E.M. (2004). Spliced-leader RNA trans splicing in a chordate, *Oikopleura dioica*, with a compact genome. Mol. Cell. Biol. *24*, 7795–7805.

Gilliam, M. (1997). Identification and roles of non-pathogenic microflora associated with honey bees. FEMS Microbiol. Lett. *155*, 1–10.

Gilliam, M., and Valentine, D.K. (1974). Enterobacteriaceae isolated from foraging worker honey bees, Apis mellifera. J. Invertebr. Pathol. *23*, 38–41.

Gladyshev, E.A., Meselson, M., and Arkhipova, I.R. (2008). Massive horizontal gene transfer in bdelloid rotifers. Science *320*, 1210–1213.

Gonçalves, C., Wisecaver, J.H., Kominek, J., Oom, M.S., Leandro, M.J., Shen, X.X., Opulente, D.A., Zhou, X., Peris, D., Kurtzman, C.P., et al. (2018). Evidence for loss and reacquisition of alcoholic fermentation in a fructophilic yeast lineage. eLife *7*, e33034.

Grabherr, M.G., Haas, B.J., Yassour, M., Levin, J.Z., Thompson, D.A., Amit, I., Adiconis, X., Fan, L., Raychowdhury, R., Zeng, Q., et al. (2011). Full-length transcriptome assembly from RNA-Seq data without a reference genome. Nat. Biotechnol. *29*, 644–652.

Gurevich, A., Saveliev, V., Vyahhi, N., and Tesler, G. (2013). QUAST: quality assessment tool for genome assemblies. Bioinformatics *29*, 1072–1075.

Haas, H., Eisendle, M., and Turgeon, B.G. (2008). Siderophores in fungal physiology and virulence. Annu. Rev. Phytopathol. *46*, 149–187.

Heinemann, J.A., and Sprague, G.F., Jr. (1989). Bacterial conjugative plasmids mobilize DNA transfer between bacteria and yeast. Nature *340*, 205–209.

Hittinger, C.T., and Carroll, S.B. (2007). Gene duplication and the adaptive evolution of a classic genetic switch. Nature *449*, 677–681.

Holt, C., and Yandell, M. (2011). MAKER2: an annotation pipeline and genome-database management tool for second-generation genome projects. BMC Bioinformatics *12*, 491.

Hooks, K.B., Delneri, D., and Griffiths-Jones, S. (2014). Intron evolution in Saccharomycetaceae. Genome Biol. Evol. *6*, 2543–2556.

Husnik, F., and McCutcheon, J.P. (2016). Repeated replacement of an intrabacterial symbiont in the tripartite nested mealybug symbiosis. Proc. Natl. Acad. Sci. USA *113*, E5416–E5424.

Husnik, F., and McCutcheon, J.P. (2018). Functional horizontal gene transfer from bacteria to eukaryotes. Nat. Rev. Microbiol. *16*, 67–79.

Husnik, F., Nikoh, N., Koga, R., Ross, L., Duncan, R.P., Fujie, M., Tanaka, M., Satoh, N., Bachtrog, D., Wilson, A.C.C., et al. (2013). Horizontal gene transfer from diverse bacteria to an insect genome enables a tripartite nested mealybug symbiosis. Cell *153*, 1567–1578.

Katoh, K., and Standley, D.M. (2013). MAFFT multiple sequence alignment software version 7: improvements in performance and usability. Mol. Biol. Evol. *30*, 772–780.

Keeling, P.J., and Palmer, J.D. (2008). Horizontal gene transfer in eukaryotic evolution. Nat. Rev. Genet. *9*, 605–618.

Keren, H., Lev-Maor, G., and Ast, G. (2010). Alternative splicing and evolution: diversification, exon definition and function. Nat. Rev. Genet. *11*, 345–355.

Khaldi, N., Collemare, J., Lebrun, M.H., and Wolfe, K.H. (2008). Evidence for horizontal transfer of a secondary metabolite gene cluster between fungi. Genome Biol. *9*, R18.

Kondo, N., Nikoh, N., Ijichi, N., Shimada, M., and Fukatsu, T. (2002). Genome fragment of Wolbachia endosymbiont transferred to X chromosome of host insect. Proc. Natl. Acad. Sci. USA *99*, 14280–14285.

Korf, I. (2004). Gene finding in novel genomes. BMC Bioinformatics *5*, 59.

Kozlov, A.M., Aberer, A.J., and Stamatakis, A. (2015). ExaML version 3: a tool for phylogenomic analyses on supercomputers. Bioinformatics *31*, 2577–2579.

Krause, D.J., Kominek, J., Opulente, D.A., Shen, X.X., Zhou, X., Langdon, Q.K., DeVirgilio, J., Hulfachor, A.B., Kurtzman, C.P., Rokas, A., and Hittinger, C.T. (2018). Functional and evolutionary characterization of a secondary metabolite gene cluster in budding yeasts. Proc. Natl. Acad. Sci. USA *115*, 11030–11035.

Lachance, M.A., Starmer, W.T., Rosa, C.A., Bowles, J.M., Barker, J.S.F., and Janzen, D.H. (2001). Biogeography of the yeasts of ephemeral flowers and their insects. FEMS Yeast Res. *1*, 1–8.

Lawrence, J.G., and Roth, J.R. (1996). Selfish operons: horizontal transfer may drive the evolution of gene clusters. Genetics *143*, 1843–1860.

Le, S.Q., and Gascuel, O. (2008). An improved general amino acid replacement matrix. Mol. Biol. Evol. *25*, 1307–1320.

Leduc, D., Battesti, A., and Bouveret, E. (2007). The hotdog thioesterase EntH (YbdB) plays a role in vivo in optimal enterobactin biosynthesis by interacting with the ArCP domain of EntB. J. Bacteriol. *189*, 7112–7126.

Machuca, A., and Milagres, A.M.F. (2003). Use of CAS-agar plate modified to study the effect of different variables on the siderophore production by *Aspergillus*. Lett. Appl. Microbiol. *36*, 177–181.

Marcet-Houben, M., and Gabaldón, T. (2010). Acquisition of prokaryotic genes by fungal genomes. Trends Genet. *26*, 5–8.

Moran, N.A., McCutcheon, J.P., and Nakabachi, A. (2008). Genomics and evolution of heritable bacterial symbionts. Annu. Rev. Genet. *42*, 165–190.

Neuvéglise, C., Marck, C., and Gaillardin, C. (2011). The intronome of budding yeasts. C. R. Biol. *334*, 662–670.

Nguyen, L.T., Schmidt, H.A., von Haeseler, A., and Minh, B.Q. (2015). IQ-TREE: a fast and effective stochastic algorithm for estimating maximum-likelihood phylogenies. Mol. Biol. Evol. *32*, 268–274.

Nikoh, N., Tanaka, K., Shibata, F., Kondo, N., Hizume, M., Shimada, M., and Fukatsu, T. (2008). Wolbachia genome integrated in an insect chromosome: evolution and fate of laterally transferred endosymbiont genes. Genome Res. *18*, 272–280.

Omelchenko, M.V., Makarova, K.S., Wolf, Y.I., Rogozin, I.B., and Koonin, E.V. (2003). Evolution of mosaic operons by horizontal gene transfer and gene displacement in situ. Genome Biol. *4*, R55.

Pelechano, V., Wei, W., and Steinmetz, L.M. (2013). Extensive transcriptional heterogeneity revealed by isoform profiling. Nature *497*, 127–131.

Pérez-Miranda, S., Cabirol, N., George-Téllez, R., Zamudio-Rivera, L.S., and Fernández, F.J. (2007). O-CAS, a fast and universal method for siderophore detection. J. Microbiol. Methods *70*, 127–131.

Pertea, M., Pertea, G.M., Antonescu, C.M., Chang, T.C., Mendell, J.T., and Salzberg, S.L. (2015). StringTie enables improved reconstruction of a transcriptome from RNA-seq reads. Nat. Biotechnol. *33*, 290–295.

Proctor, R.H., Van Hove, F., Susca, A., Stea, G., Busman, M., van der Lee, T., Waalwijk, C., Moretti, A., and Ward, T.J. (2013). Birth, death and horizontal transfer of the fumonisin biosynthetic gene cluster during the evolutionary diversification of *Fusarium*. Mol. Microbiol. *90*, 290–306.

Richards, T.A., Dacks, J.B., Jenkinson, J.M., Thornton, C.R., and Talbot, N.J. (2006). Evolution of filamentous plant pathogens: gene exchange across eukaryotic kingdoms. Curr. Biol. *16*, 1857–1864.

Richards, T.A., Leonard, G., Soanes, D.M., and Talbot, N.J. (2011). Gene transfer into the fungi. Fungal Biol. Rev. *25*, 98–110.

Richards, T.A., Soanes, D.M., Jones, M.D.M., Vasieva, O., Leonard, G., Paszkiewicz, K., Foster, P.G., Hall, N., and Talbot, N.J. (2011). Horizontal gene transfer facilitated the evolution of plant parasitic mechanisms in the oomycetes. Proc. Natl. Acad. Sci. USA *108*, 15258–15263.

Rosa, C.A., and Lachance, M.A. (1998). The yeast genus Starmerella gen. nov. and Starmerella bombicola sp. nov., the teleomorph of Candida bombicola (Spencer, Gorin & Tullock) Meyer & Yarrow. Int. J. Syst. Evol. Microbiol. *48*, 1413–1417.

Rosa, C.A., Lachance, M.A., Silva, J.O.C., Teixeira, A.C.P., Marini, M.M., Antonini, Y., and Martins, R.P. (2003). Yeast communities associated with stingless bees. FEMS Yeast Res. *4*, 271–275.

Routh, A., Domitrovic, T., and Johnson, J.E. (2012). Host RNAs, including transposons, are encapsidated by a eukaryotic single-stranded RNA virus. Proc. Natl. Acad. Sci. USA *109*, 1907–1912.

Scharf, D.H., Heinekamp, T., and Brakhage, A.A. (2014). Human and plant fungal pathogens: the role of secondary metabolites. PLoS Pathog. *10*, e1003859.

Seo, S.W., Kim, D., Latif, H., O'Brien, E.J., Szubin, R., and Palsson, B.O. (2014). Deciphering Fur transcriptional regulatory network highlights its complex role beyond iron metabolism in *Escherichia coli*. Nat. Commun. *5*, 4910.

Sheftel, A., Stehling, O., and Lill, R. (2010). Iron-sulfur proteins in health and disease. Trends Endocrinol. Metab. *21*, 302–314.

Shen, X.X., Zhou, X., Kominek, J., Kurtzman, C.P., Hittinger, C.T., and Rokas, A. (2016). Reconstructing the backbone of the Saccharomycotina yeast phylogeny using genome-scale data. G3 (Bethesda) *6*, 3927–3939.

Shen, X.X., Opulente, D.A., Kominek, J., Zhou, X., Steenwyk, J.L., Buh, K.V., Haase, M.A.B., Wisecaver, J.H., Wang, M., Doering, D.T., et al. (2018). Tempo and mode of genome evolution in the budding yeast subphylum. Cell *175*, 1533–1545.

Simão, F.A., Waterhouse, R.M., Ioannidis, P., Kriventseva, E.V., and Zdobnov, E.M. (2015). BUSCO: assessing genome assembly and annotation completeness with single-copy orthologs. Bioinformatics *31*, 3210–3212.

Skaar, E.P. (2010). The battle for iron between bacterial pathogens and their vertebrate hosts. PLoS Pathog. *6*, e1000949.

Slot, J.C., and Rokas, A. (2010). Multiple GAL pathway gene clusters evolved independently and by different mechanisms in fungi. Proc. Natl. Acad. Sci. USA *107*, 10136–10141.

Slot, J.C., and Rokas, A. (2011). Horizontal transfer of a large and highly toxic secondary metabolic gene cluster between fungi. Curr. Biol. *21*, 134–139.

Soucy, S.M., Huang, J., and Gogarten, J.P. (2015). Horizontal gene transfer: building the web of life. Nat. Rev. Genet. *16*, 472–482.

Spieth, J., Brooke, G., Kuersten, S., Lea, K., and Blumenthal, T. (1993). Operons in *C. elegans*: polycistronic mRNA precursors are processed by trans-splicing of SL2 to downstream coding regions. Cell *73*, 521–532.

Stairs, C.W., Eme, L., Brown, M.W., Mutsaers, C., Susko, E., Dellaire, G., Soanes, D.M., van der Giezen, M., and Roger, A.J. (2014). A SUF Fe-S cluster biogenesis system in the mitochondrion-related organelles of the anaerobic protist Pygsuia. Curr. Biol. *24*, 1176–1186.

Stamatakis, A. (2014). RAxML version 8: a tool for phylogenetic analysis and post-analysis of large phylogenies. Bioinformatics *30*, 1312–1313.

Stanke, M., Diekhans, M., Baertsch, R., and Haussler, D. (2008). Using native and syntenically mapped cDNA alignments to improve de novo gene finding. Bioinformatics *24*, 637–644.

Stefanini, I., Dapporto, L., Berná, L., Polsinelli, M., Turillazzi, S., and Cavalieri, D. (2016). Social wasps are a *Saccharomyces* mating nest. Proc. Natl. Acad. Sci. USA *113*, 2247–2251.

Sutak, R., Lesuisse, E., Tachezy, J., and Richardson, D.R. (2008). Crusade for iron: iron uptake in unicellular eukaryotes and its significance for virulence. Trends Microbiol. *16*, 261–268.

Ter-Hovhannisyan, V., Lomsadze, A., Chernoff, Y.O., and Borodovsky, M. (2008). Gene prediction in novel fungal genomes using an ab initio algorithm with unsupervised training. Genome Res. *18*, 1979–1990.

Toth, I.K., Pritchard, L., and Birch, P.R.J. (2006). Comparative genomics reveals what makes an enterobacterial plant pathogen. Annu. Rev. Phytopathol. *44*, 305–336.

Tsaousis, A.D., Ollagnier de Choudens, S., Gentekaki, E., Long, S., Gaston, D., Stechmann, A., Vinella, D., Py, B., Fontecave, M., Barras, F., et al. (2012). Evolution of Fe/S cluster biogenesis in the anaerobic parasite *Blastocystis*. Proc. Natl. Acad. Sci. USA *109*, 10426–10431.

Van Doren, K., and Hirsh, D. (1990). mRNAs that mature through trans-splicing in *Caenorhabditis elegans* have a trimethylguanosine cap at their 5′ termini. Mol. Cell. Biol. *10*, 1769–1772.

Vandenberghe, A.E., Meedel, T.H., and Hastings, K.E.M. (2001). mRNA 5′-leader trans-splicing in the chordates. Genes Dev. *15*, 294–303.

Wandersman, C., and Delepelaire, P. (2004). Bacterial iron sources: from siderophores to hemophores. Annu. Rev. Microbiol. *58*, 611–647.

Watanabe, K., and Sato, M. (1998). Plasmid-mediated gene transfer between insect-resident bacteria, *Enterobacter cloacae*, and plant-epiphytic bacteria, *Erwinia herbicola*, in guts of silkworm larvae. Curr. Microbiol. *37*, 352–355.

Watanabe, K., Hara, W., and Sato, M. (1998). Evidence for growth of strains of the plant epiphytic bacterium *Erwinia herbicola* and transconjugation among the bacterial strains in guts of the silkworm *Bombyx mori*. J. Invertebr. Pathol. *72*, 104–111.

Wisecaver, J.H., and Rokas, A. (2015). Fungal metabolic gene clusters-caravans traveling across genomes and environments. Front. Microbiol. *6*, 161.

Wisecaver, J.H., Alexander, W.G., King, S.B., Hittinger, C.T., and Rokas, A. (2016). Dynamic evolution of nitric oxide detoxifying flavohemoglobins, a family of single-protein metabolic modules in bacteria and eukaryotes. Mol. Biol. Evol. *33*, 1979–1987.

Wu, T.D., and Nacu, S. (2010). Fast and SNP-tolerant detection of complex variants and splicing in short reads. Bioinformatics *26*, 873–881.

Yurchenko, T., Ševčíková, T., Strnad, H., Butenko, A., and Eliáš, M. (2016). The plastid genome of some eustigmatophyte algae harbours a bacteria-derived six-gene cluster for biosynthesis of a novel secondary metabolite. Open Biol. *6*, 160249.

Yurchenko, T., Ševčíková, T., Přibyl, P., El Karkouri, K., Klimeš, V., Amaral, R., Zbránková, V., Kim, E., Raoult, D., Santos, L.M.A., and Eliáš, M. (2018). A gene transfer event suggests a long-term partnership between eustigmatophyte algae and a novel lineage of endosymbiotic bacteria. ISME J. *12*, 2163–2175.

Zhou, X., Peris, D., Kominek, J., Kurtzman, C.P., Hittinger, C.T., and Rokas, A. (2016). In silico whole genome sequencer & analyzer (iWGS): a computational pipeline to guide the design and analysis of de novo genome sequencing studies. G3 (Bethesda) *6*, 3655–3662.

STAR★METHODS

KEY RESOURCES TABLE

REAGENT or RESOURCE	SOURCE	IDENTIFIER
Bacterial and Virus Strains		
E. cloni 10G Chemically Competent Cells	Lucigen	Cat#60107-2
Escherichia coli MG1655	Blattner et al., 1997	ATCC: 700926
Chemicals, Peptides, and Recombinant Proteins		
Enterobactin	Sigma Aldrich	Cat#E3910
Chromeazurol S	MP Biomedicals, LLC	Cat#154982
Ferric chloride hexahydrate	VWR	Cat#0682-500G
Hydrochloric acid	J.T. Baker	Cat#9535-05
Hexadecyltrimethylammonium bromide	Sigma Aldrich	Cat#H6269
Phusion High-Fidelity DNA Polymerase	New England Biolabs	Cat#M0530S
Taq DNA Polymerase with Standard *Taq* Buffer	New England Biolabs	Cat#M0273
Exonuclease I	New England Biolabs	Cat#M0293L
Antarctic Phosphatase	New England Biolabs	Cat#M0289L
25:24:1 Phenol:Chloroform:Isoamyl Alcohol	Sigma Aldrich	Cat#P2069
RNase A	VWR Life Science	Cat##97064-064
Critical Commercial Assays		
RNA Clean & Concentrator Kit	Zymo Research	Cat#R1017; Cat#R1018
Qubit RNA Assay Kit	Thermo Fisher	Cat#Q32852
Qubit dsDNA Assay Kit	Thermo Fisher	Cat#Q32853
NEBNext Poly(A) mRNA Magnetic Isolation Module	New England Biolabs	Cat#E7490
NEBNext Ultra Directional RNA Library Prep Kit	New England Biolabs	Cat#E7420
FirstChoice RLM-RACE Kit	Invitrogen	Cat#AM1700
Zymoclean Gel DNA Recovery Kit	Zymo Research	Cat#D4002
pCR-Blunt II-TOPO Kit	Thermo Fisher	Cat#450031
BigDye Terminator Cycle Sequencing Kit	Applied Biosystems	Cat#4337455
ZR Plasmid Miniprep	Zymo Research	Cat#D4016
AxyPrep Mag DyeClean Beads	Fisher Scientific	Cat#14-223-163
NEBNext Ultra DNA Library Prep Kit	New England Biolabs	Cat#E7370L
AxyPrep Mag PCR Beads	Fisher Scientific	Cat#14-223-152
Deposited Data		
Raw DNA reads, raw RNA reads and whole genome assembly data	This paper	BioProject: PRJNA396763
Experimental Models: Organisms/Strains		
Saccharomyces cerevisiae	Hittinger and Carroll, 2007	FM1282
Kluyveromyces lactis	CBS	CBS 2359
Tortispora caseinolytica	NRRL	NRRL Y-17796^T
Yarrowia keelungensis	NRRL	NRRL Y-63742^T
Yarrowia deformans	NRRL	NRRL Y-321^T
Yarrowia lipolytica	NRRL	NRRL YB-423^T
Blastobotrys adeninivorans	NRRL	NRRL Y-17592
Sugiyamaella lignohabitans	NRRL	NRRL YB-1473^T
Wickerhamiella (Candida) infanticola	NRRL	NRRL Y-17858^T
Wickerhamiella (Candida) hasegawae	JCM	JCM 12559^T
Wickerhamiella (Candida) pararugosa	NRRL	NRRL Y-17089^T

(*Continued on next page*)

Continued

REAGENT or RESOURCE	SOURCE	IDENTIFIER
Wickerhamiella cacticola	NRRL	NRRL Y-27362^T
Wickerhamiella occidentalis	NRRL	NRRL Y-27364
Wickerhamiella (Candida) versatilis	NRRL	NRRL Y-6652^T
Wickerhamiella domercqiae	NRRL	NRRL Y-6692^T
Starmerella (Candida) gropengiesseri	NRRL	NRRL Y-17142^T
Starmerella (Candida) tilneyi	CBS	CBS 8794^T
Starmerella (Candida) sorbosivorans	CBS	CBS 8768^T
Starmerella (Candida) geochares	NRRL	NRRL Y-17073^T
Starmerella (Candida) vaccinii	NRRL	NRRL Y-17684^T
Starmerella (Candida) davenportii	CBS	CBS 9069^T
Starmerella (Candida) ratchasimensis	CBS	CBS 10611^T
Starmerella (Candida) apicola	NRRL	NRRL Y-2481^T
Starmerella (Candida) riodocensis	NRRL	NRRL Y-27859^T
Starmerella (Candida) kuoi	NRRL	NRRL Y-27208^T
Starmerella bombicola	NRRL	NRRL Y-17069^T
Lipomyces starkeyi	NRRL	NRRL Y-11557^T
Oligonucleotides		
NEBNext Multiplex Oligos for Illumina	New England Biolabs	Cat#E7335, E7500
M13 Forward (−20) and Reverse primers	Included in pCR-Blunt II-TOPO Kit	N/A
RACE Primers	This study	See Table S3
Software and Algorithms		
BLAST+ suite v2.2.28	Altschul et al., 1990	ftp://ftp.ncbi.nlm.nih.gov/blast/executables/blast+/
iWGS v1.01	Zhou et al., 2016	https://github.com/zhouxiaofan1983/iWGS
Quast v4.4	Gurevich et al., 2013	https://github.com/ablab/quast
Maker v2.31.8	Holt and Yandell, 2011	http://yandell-lab.org/software/maker.html
GeneMark-ES v4.10	Ter-Hovhannisyan et al., 2008	http://topaz.gatech.edu/GeneMark/license_download.cgi
Augustus v3.2.1	Stanke et al., 2008	http://bioinf.uni-greifswald.de/augustus/downloads/
SNAP release 2006-07-28	Korf 2004	https://github.com/KorfLab/SNAP
BUSCO v3	Simão et al., 2015	https://busco.ezlab.org/
MAFFT v7	Katoh and Standley, 2013	https://mafft.cbrc.jp/alignment/software/
RAxML v8	Stamatakis 2014	https://github.com/stamatak/standard-RAxML
ExaML v3.0.18	Kozlov et al., 2015	https://github.com/stamatak/ExaML
IQTREE v1.5.4	Nguyen et al., 2015	http://www.iqtree.org/
GSNAP in GMAP release date 2017-05-08	Wu and Nacu, 2010	http://research-pub.gene.com/gmap/
Trinity v2.4.0	Grabherr et al., 2011	https://github.com/trinityrnaseq/trinityrnaseq/wiki
StringTie v1.3.3b	Pertea et al., 2015	https://github.com/gpertea/stringtie
MEME and TOMTOM in MEME suite v5.0.3	Bailey et al., 2009	http://meme-suite.org/doc/download.html
Other		
425-600 μm Glass beads, acid-washed	Sigma Aldrich	Cat#G8772-1KG
E220evolution Focused-ultrasonicator	Covaris	N/A

CONTACT FOR REAGENT AND RESOURCE SHARING

Further information and requests for resources and reagents should be directed to and will be fulfilled by the Lead Contact, Chris Todd Hittinger (cthittinger@wisc.edu).

EXPERIMENTAL MODEL AND SUBJECT DETAILS

Yeast strains were obtained from the USDA Agricultural Research Service (ARS) NRRL Culture Collection in Peoria, Illinois, USA. All sequenced strains have been publicly deposited in the NRRL or CBS. All yeast strains were struck for single colonies from a glycerol freezer stock to YPD (1% w/v yeast extract, 2% w/v peptone, 2% w/v dextrose) agar plates and grown at either room temperature or 30°C until visible colonies formed. Culturing conditions prior to RNA isolation and HPLC sample preparation can be found in the relevant Method Details sections. Strain identifiers and other information for each yeast species can be found in either the Key Resources Table or Table S1.

METHOD DETAILS

Genome sequencing

Genomic DNA (gDNA) isolation and Illumina library prep was done as described previously (Shen et al., 2018). Briefly, cells were grown to saturation in YPD broth, collected by centrifugation with approximately 500 μL 0.5 mm acid-washed beads (Sigma #G8772), and resuspended in DNA lysis buffer (10 mM Tris, 1 mM EDTA, 100 mM NaCl, 1% SDS, 2% Triton X-100 in water). Then, samples were extracted twice with 25:24:1 phenol:chloroform:isoamyl alcohol (Sigma #P2069), precipitated overnight at −80°C in 100% ethanol, collected by centrifugation, washed twice with 70% ethanol, dissolved in 10 mM Tris-Cl (pH 8), and treated with RNase A (VWR #97064-064) for 30 minutes at 37°C. gDNA was then sonicated using a (Covaris E220 Focused-ultrasonicator); followed by end-repair, adaptor ligation and size selection with the NEBNext Ultra DNA Library Prep kit (NEB #E7370L), which was performed according to the manufacturer's protocol except that Axygen AxyPrep Mag PCR beads (Fisher Sci #14-223-152) were used instead of Beckman Coulter AMPure XP beads. Libraries were then submitted for 2x250 bp sequencing on an Illumina HiSeq 2500 instrument.

RNA sequencing

Cells were grown in quadruplicates for either 3 or 6 days on YPD agar, and RNA was extracted using the hot acid phenol protocol (Chomczynski and Sacchi, 1987). Briefly, cells were scraped off of agar plates and flash frozen in a dry ice-ethanol bath. Then, cells were resuspended in TES buffer (10 mM Tris, 10 mM EDTA, 0.5% SDS in water), and added to one volume of 5:1 acid phenol:chloroform. Lysates were then incubated at 70°C for one hour with vortexing every 15 minutes. Then, lysates were extracted twice with one volume of 5:1 phenol:chloroform each and once with chloroform. The aqueous phase of the final chloroform extraction was added to a solution consisiting of 2.5 volumes of 95%–100% ethanol and 0.1 volumes of 3 M sodium acetate and was placed at −80°C overnight to precipitate the RNA. RNA pellets were then collected by centrifugation, washed twice with 1 volume of 70% ethanol each, and resuspended in RNase-free water. Purified RNA was then treated with DNase to remove any residual DNA prior to treatment with the RNA Clean & Concentrator kit (Zymo Research #R1017, R1018). Total RNA yields were quantified with the Qubit RNA Assay Kit (Thermo Fisher). Next, mRNA was isolated using the NEBNext Poly(A) mRNA Magnetic Isolation Module (NEB #E7490) and prepared into strand-specific Illumina libraries using the NEBNext Ultra Directional RNA Library Prep Kit (NEB #E7420) and the NEBNext Multiplex Oligos for Illumina (New England Biolabs #E7335, E7500). Library quality was assessed by gel electrophoresis and with the Qubit dsDNA Kit (Thermo Fisher) prior to submission for 2x125 paired-end sequencing with an Illumina HiSeq 2500 instrument.

Mapping transcript ends by 3′ and 5′ RLM-RACE

5′ RNA Ligase-Mediated Rapid Amplification of cDNA Ends (RLM-RACE) and 3′ RACE were carried out using the FirstChoice RLM-RACE Kit (Invitrogen #AM1700), as directed in the kit instructions. Gene-specific outer and inner nested primers used to amplify RACE products were designed to match the annealing temperatures of the RACE outer and inner PCR primers, respectively, with minimal hairpin, self-dimer, and hetero-dimer affinities (Table S3). RACE PCR master mixes were assembled as directed in the kit manual, except we used 1.25 U of Phusion High-Fidelity DNA Polymerase (NEB #M0530S) with HF Buffer. Cycling for nested RACE PCR was carried out under the following conditions: 98°C for 1:00 min; then 35 cycles of 98°C for 10 s, primer-specific annealing temperature for 30 s (temperatures indicated in Table S3), and 72°C for 2:30 min; followed by a final extension at 72°C for 5:00 min, and hold at 15°C.

Cloning and confirmation of RACE products

Products from the inner nested RACE PCR were run on a 1% agarose gel and visualized by staining with ethidium bromide. Bands corresponding to distinct RACE PCR products were cut out, extracted with the Zymoclean Gel DNA Recovery Kit (Zymo Research #D4002), and cloned by TOPO blunt-end cloning into pCR-Blunt II-TOPO (Thermo Fisher #450031). The resulting plasmids were transformed into *E. coli* 10G Chemically Competent Cells (Lucigen #60107-2) and plated onto LB Agar with 50 μg/mL kanamycin. Resulting colonies were inoculated into LB Broth with 50 μg/mL kanamycin sulfate to incubate overnight at 37°C. Their plasmid inserts were then Sanger sequenced by BigDye Terminator Cycle Sequencing (Applied Biosystems) using the M13 forward (−20) or reverse primers, either by miniprep extraction (Zymo Research #D4016) or by colony PCR followed by treatment with Exonuclease I/Antarctic Phosphatase (NEB #M0293L, #M0289L). Excess dideoxy-terminators were removed using AxyPrep Mag DyeClean beads (Fisher Scientific #14-223-163). Colony PCR was conducted with *Taq* DNA Polymerase with Standard Taq Buffer (NEB #M0273) as

follows: 10:00 min at 95°C; then 35 cycles of 95°C for 30 s, 44°C for 30 s, and 68°C for 1:00 min; followed by a final extension of 68°C for 5:00 min, and hold at 15°C.

Microbial culturing and O-CAS assays

Low-iron synthetic complete (SC) medium consisted of 5 g/L ammonium sulfate, 1.7 g/L Yeast Nitrogen Base (without amino acids, carbohydrates, ammonium sulfate, ferric chloride, or cupric sulfate), 2 g/L complete dropout mix, 2% dextrose (added after autoclaving), and 200 nM cupric sulfate. M9 minimal medium consisted of 0.4% glucose, 2 mM magnesium sulfate, 100 μM calcium dichloride, and 1x M9 salts (added as a 5x stock solution consisting of 64 g/L dibasic sodium phosphate heptahydrate, 15 g/L monobasic potassium phosphate, 2.5 g/L sodium chloride, and 5 g/L ammonium chloride in deionized water).

The chromeazurol S overlay (O-CAS) assay was carried out as previously described (Pérez-Miranda et al., 2007), with some modifications. Specifically, 10X CAS Blue Dye was made by combining the following: 50 mL Solution 1 (60 mg chromeazurol S dissolved in 50 mL deionized H_2O), 9 mL Solution 2 (13.5 mg ferric chloride hexahydrate dissolved in 50 mL 10 mM hydrochloric acid), and 40 mL Solution 3 (73 mg hexadecyltrimethylammonium bromide (HDTMA) in 40 mL deionized H_2O). Separately, 15.12 g PIPES (free acid) was added to 425 mL deionized water and adjusted to a pH of approximately 6.8 with 2.46 g sodium hydroxide. 4.5 g agarose was added as a solidifying agent, and the resulting solution was brought up to 450 mL with deionized water in a 1-L Erlenmeyer flask. To make the CAS overlay, the agarose-PIPES solution was heated to melt the agarose and added in a ratio of 9:1 to 10X CAS Blue Dye, and 6 mL of the resulting O-CAS solution were overlaid onto low-iron SC plates.

Yeast strains were grown to saturation in 3 mL YPD medium at 30°C on a rotating culture wheel, centrifuged at 3000 rpm for 5 minutes to collect the cells, and resuspended in 3 mL deionized water. A volume of 5 μL of the resulting cell suspension was spotted onto 60 mm diameter plates containing low-iron SC medium using agarose (1% w/v) as a gelling agent and incubated at 30°C for 7 days before adding 6 mL of O-CAS solution. *E. coli* cells were grown overnight in M9 minimal medium at 37°C, and 5 μL of culture was spotted onto low-iron SC plates that had already been overlaid with 6 mL of O-CAS solution and allowed to dry for at least 1 hour. Pictures of yeast colonies were taken 2 days after the O-CAS was poured, while *E. coli* colonies were photographed 5 days after the O-CAS was poured. With exposure and focus lock enabled, pictures were taken of the plates set on top of a miniature white light trans-illuminator placed under a gel-imaging dark box.

HPLC analysis of yeast culture extracts

Yeasts were grown on YPD plates until colonies formed; a colony was inoculated into low-iron SC medium with either 2% dextrose or 2% glycerol as a carbon source, as indicated (Table S4), and the resulting culture was incubated at 30°C for either 3 or 6 days, as indicated. The spent medium was then centrifuged, and the supernatant was filtered through a 0.2 μm nylon filter directly into a 2 mL LC vial. The filtered samples were analyzed for the presence of enterobactin on a Shimadzu LCMS8040 using 50 μL injections of the filtered yeast culture. Sample to sample carryover was minimized by rinsing the needle assembly and using two blank injections of 10 μL isopropanol between samples. The mobile phase was a binary gradient of acetonitrile and water, pumped at 0.7 mL/min through a Phemonenex Kinetex 5μ XB-C18 column (P/N: 00G-4605-E0, 100 Å, 250′4.6 mm) and heated at 60°C.

The mobile phase was held at 0% acetonitrile for 0.2 minutes, then ramped to 100% acetonitrile over 3.05 minutes, and held there for 2.25 minutes to wash the column. The mobile phase was then ramped back to 0% acetonitrile over 0.5 minutes and held at 0% acetonitrile for 4 minutes to reset the column's initial condition. The eluent was diverted to waste for the first 2 minutes to minimize salt buildup on the ion source. After 2 minutes, the eluent flowed through a PDA detector scanning from 190–400 nm and into the MS ionization source operating in DUIS (ESI/APCI) mode with 2.5 L/min nebulizing gas, 20 L/min drying gas, 300°C DL temperature, and 400°C heat block. The MS scanned the ions in negative mode from 200–1000 *m/z*, and monitored three MRM transitions (668→178, 668→222, and 668→445, Table S4) with argon collision gas at 230 kPa. The retention time and relative intensities of the three MRM transitions were determined using an enterobactin standard (Sigma Aldrich #E3910, Figure S4). The results of the yeast strain screening are presented in Figure 3 and Table S4.

QUANTIFICATION AND STATISTICAL ANALYSIS

Identification of iron metabolism genes

Amino acid sequences of proteins known to be involved in iron uptake and storage were used as BLASTP and TBLASTN v2.2.28+ (Altschul et al., 1990) queries against genomes and proteomes of a broad range of dikaryon fungal species (see Table S1). The genomic data was obtained from GenBank, as well as from draft genome assemblies generated for 20 strains by the RIKEN BioResource Center and RIKEN Center for Life Science Technologies through the Genome Information Upgrading Program of the National Bio-Resource Project of the MEXT. *S. cerevisiae* homologs were used, except for: the fungal hydroxamate-class siderophore biosynthesis proteins, which came from *A. nidulans;* the bacterial catecholate-class siderophore biosynthesis proteins, which came from *E. coli;* and the iron-responsive GATA factor sequences, which came from *A. nidulans* (SreA), *Ustilago maydis* (Urbs1), *Phanerochate chrysosporium* (SreP), *Neurospora crassa* (Sre), *Candida albicans* (Sfu1), and *Schizosaccharomyces pombe* (Fep1). Identification of *entA-entF* genes in bacterial genomes was performed using *E. coli* protein sequences as queries for BLASTP and TBLASTN to search 1,382 Enterobacteriales genomes and proteomes downloaded from GenBank. Only genes from the 207 genomes where all six genes could be identified at E-value cutoff of 1E-10 were considered for further phylogenetic analyses.

Genome assembly and annotation

To generate whole-genome assemblies, Illumina reads were used as input to the meta-assembler pipeline iWGS v1.01 (Zhou et al., 2016). Briefly, this pipeline performed quality-based read trimming, followed by k-mer length optimization, and used a range of state-of-the-art assemblers to generate multiple genome assemblies. Assembly quality was assessed using QUAST v4.4 (Gurevich et al., 2013), and the best assembly for each species was chosen based on the N_{50} statistic. ORFs were annotated in genomes using the MAKER pipeline v2 (Holt and Yandell, 2011) and the GeneMark-ES v4.10 (Ter-Hovhannisyan et al., 2008), Augustus v3.2.1 (Stanke et al., 2008), and SNAP (release 2006-07-28) (Korf, 2004) gene predictors.

Phylogenetic reconstruction and tests

The species phylogeny was obtained by analyzing conserved single-copy fungal orthologs by using a previously described phylogenomic approach (Shen et al., 2016). Briefly, sequences of conserved, single-copy orthologous genes were identified in the genome assemblies using the BUSCO v3 software (Simão et al., 2015), single-copy BUSCO genes shared by at least 80% of species were aligned using MAFFT v7 (Katoh and Standley, 2013), and these orthologs were used for maximum-likelihood phylogenetic reconstruction with RAxML v8 (Stamatakis 2014). The reconstruction was performed under the LG model of amino acid substitution (Le and Gascuel, 2008) with empirical amino acid frequencies, four gamma distribution rate categories to estimate rate heterogeneity, and 100 rapid bootstrap pseudoreplicates. A concatenated super-alignment of all genes was also used for phylogenetic reconstruction by running ExaML v3.0.18 (Kozlov et al., 2015) under the JTT substitution matrix (chosen by the built-in maximum-likelihood model selection), per-site rate heterogeneity model with median approximation of the GAMMA rates, and with memory saving option for gappy alignments turned on. Constrained phylogeny reconstructions were conducted in RAxML through the "-g" option, and the AU and SH topology tests were performed with IQ-TREE v1.5.4 (Nguyen et al., 2015) using 10,000 bootstrap pseudoreplicates.

Three evolutionary scenarios were considered to explain the course of the horizontal transfer event: (I) single-source, single-target; (II) single-source, multiple-targets; and (III) multiple-sources. Each of them predicted specific phylogenetic patterns. Scenario I predicted that the yeast sequences would form a strongly supported monophyletic group with a consistent internal topology. Scenario II predicted that yeast sequences would form a strongly supported monophyletic group but not follow a consistent internal topology. Scenario III predicted that yeast sequences would not form a monophyletic group. To first establish whether there was a single (I & II) or multiple donor species (III), we determined whether the yeast sequences created a strongly supported monophyletic group within the Enterobacteriales phylogeny. The monophyletic base of the yeast clade had full bootstrap support, but we used the AU test again to compare the phylogeny constrained so that all 12 yeast taxa formed a separate monophyletic group versus 12 alternative phylogenies constrained so that 11 yeast taxa were monophyletic, and the remaining single taxon could be placed freely on the tree. For all six genes, every phylogeny tested was within the 95% confidence interval of the best-supported phylogeny and thus showed no statistical difference, strongly supporting the single origin scenario (Figure 2D; Table S2). To determine whether the transfer happened into an ancestor of the W/S clade species studied (scenario I) or into various yeast lineages independently (scenario II), we looked at the topology of the yeast clade. Under the first scenario, yeast sequences would recapitulate a consistent, well-supported phylogeny, whereas under the second scenario, the phylogenetic signal would be weak, and the topology would be poorly supported. Bootstrap supports at the internal nodes in the five- and six-gene phylogenies were high (Figures 2A and 2B), which indicated consistent phylogenetic signal in the alignments. We next compared the unconstrained ML phylogenies versus phylogenies constrained so that the yeast sequences follow the topology of the five-gene concatenation (5G), and the AU test again showed that there was no statistically significant difference between them, which we took as indication that the transfer most likely happened from a single ancestral Enterobacteriales lineage into the ancestor of the 12 yeast taxa (Figure 2D; Table S2). SH tests had less statistical power but produced fully concordant results with the same constraints (Table S2).

RNA-Seq analysis

Reads were mapped to their respective genome assemblies using GSNAP (Wu and Nacu, 2010) from the GMAP package (release date 2017-05-08) with the novel splicing site search option enabled. De novo transcriptome assembly was performed using the Trinity pipeline v2.4.0 (Grabherr et al., 2011), which was run in the RF strand-specific mode with the jaccard-clip option enabled. Transcript abundances of siderophore biosynthesis genes were estimated using StringTie v1.3.3b (Pertea et al., 2015).

Evidence of transcriptional processing was evaluated by inspecting parts of the RNA-Seq reads that were soft-clipped from the ends of reads during the mapping step. 3′ ends were inspected for evidence of poly(A) tails of at least three consecutive As or Ts, which were not encoded in the genome. The power of such analysis is limited by the fact that only small fraction of reads (~0.05%) are expected to be initiated using the $(A)_6$ or $(T)_6$ primers, which increases the rate of false negative results, but true positive results remain unaffected. With this caveat, we note that evidence of poly(A) tails was not detected from the *W. versatilis entE, entA,* and *entH* genes. 5′ ends were inspected for presence of common sequences, encoded elsewhere in the genome, which could have been indicative of splicing leaders (in case of *trans*-splicing) or cassette exons (in case of alternative cis-splicing).

Identification of enriched motifs in promoters

Motifs enriched in the promoter regions of the 12 species that harbor the siderophore biosynthesis genes were identified and analyzed using the MEME-suite v5.0.3 (Bailey et al., 2009). Sequences of 100, 200, 300, 400, and 500 nucleotides upstream of the start codon of each *ent* gene were extracted and searched for statistically enriched DNA motifs of 10, 15, or 20 bases in length

using the program MEME. The program was run on both the sense and antisense strands (option "-revcomp"), looking for any number of motif repetitions (option "-mod anr"), extracting up to 20 motifs (option "-nmotifs 20") or up to the E-value of 1e-3 (option "-evt 1e-3"). Identified motifs were then queried against the YEASTRACT database of experimentally determined transcription factor binding sites using the program TOMTOM, run with default options.

HPLC analysis of yeast culture extracts

Yeast strains were determined to be positive for the production of enterobactin by HPLC-MS/MS if the chromatograms from at least four of the six biological cultures (see Table S4) were found to have an enterobactin peak (correct retention time, all three MRM transitions with relative intensities of 30% the authentic standard, and > 5:1 signal-to-noise in the MRM chromatogram of the 668 → 178 transition).

DATA AND SOFTWARE AVAILABILITY

Raw DNA and RNA sequencing data were deposited in GenBank under Bioproject ID PRJNA396763 (https://www.ncbi.nlm.nih.gov/bioproject/PRJNA396763). Whole Genome Shotgun assemblies have been deposited at DDBJ/ENA/GenBank under the accessions NRDR00000000-NREI00000000. Genome-specific accessions are listed in Table S1.

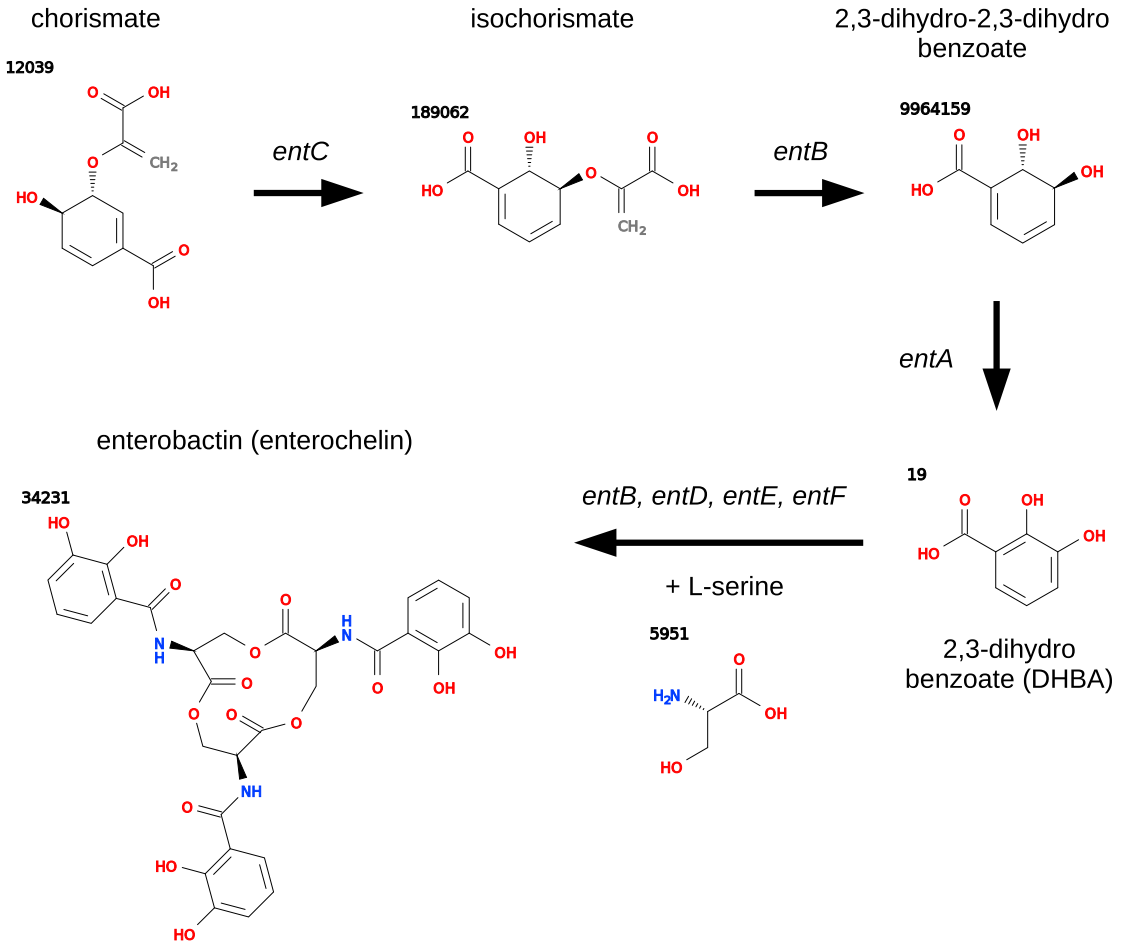

Figure S1. Enterobactin Biosynthesis from Chorismate, Related to Figure 1

Genes involved at each biosynthesis step are marked above arrows. Intermediates of the final biosynthesis step have not yet been determined. PubChem IDs of individual chemical structures are marked in bold. Chorismate biosynthesis is broadly conserved because it is a key compound in the shikimate pathway that is involved in biosynthesis of aromatic amino acids. *entH* encodes a proofreading thioesterase whose activity is not required for the production of enterobactin and related catecholate-class siderophores.

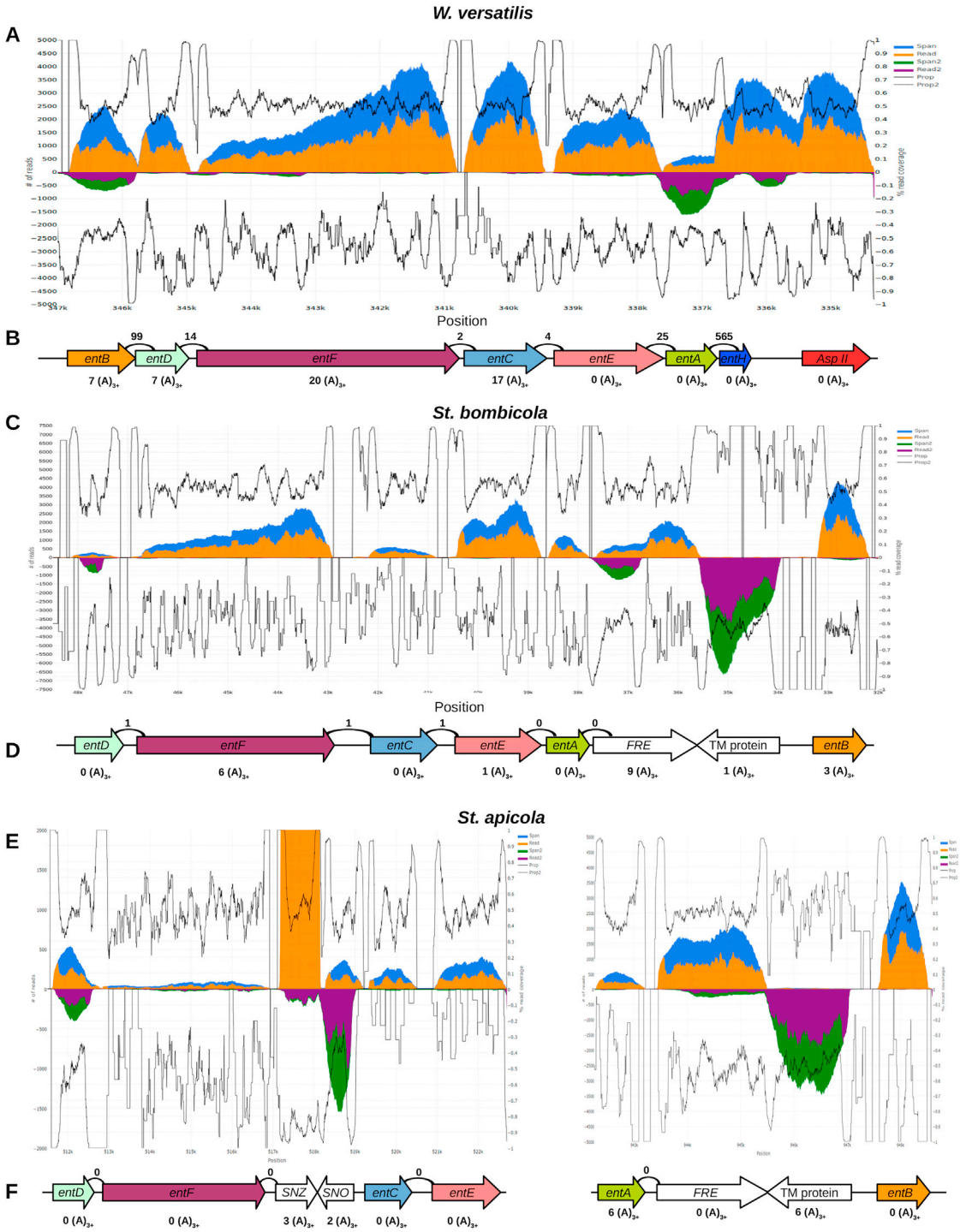

Figure S2. Transcriptomics of the Siderophore Biosynthesis Genes in *W. versatilis*, *St. bombicola*, and *St. apicola*, Related to Figure 4

(A, C, E) RNA-seq coverage of the genomic region containing siderophore biosynthesis genes in (A) *W. versatilis*, (C) *St. bombicola*, and (E) *St. apicola*. The orange area indicates per-base coverage by RNA-Seq reads (read coverage). The blue area indicates per-base cumulative coverage by RNA-Seq reads and inserts between read-pairs (span coverage). The purple area indicates read coverage of the opposite strand. The green area indicates span coverage of the opposite strand. The black lines indicate the ratios of the read coverage over the span coverage data for the relevant strand. (B, D, F) Diagrams of siderophore biosynthesis genes in the genomes of (B) *W. versatilis*, (D) *St. bombicola*, and (F) *St. apicola*, drawn to scale, including a gene predicted to encode a bacterial class II asparaginase in *W. versatilis*. Counts above indicate read-pairs crossmapping between genes. Counts below indicate reads containing putative poly(A) tails.

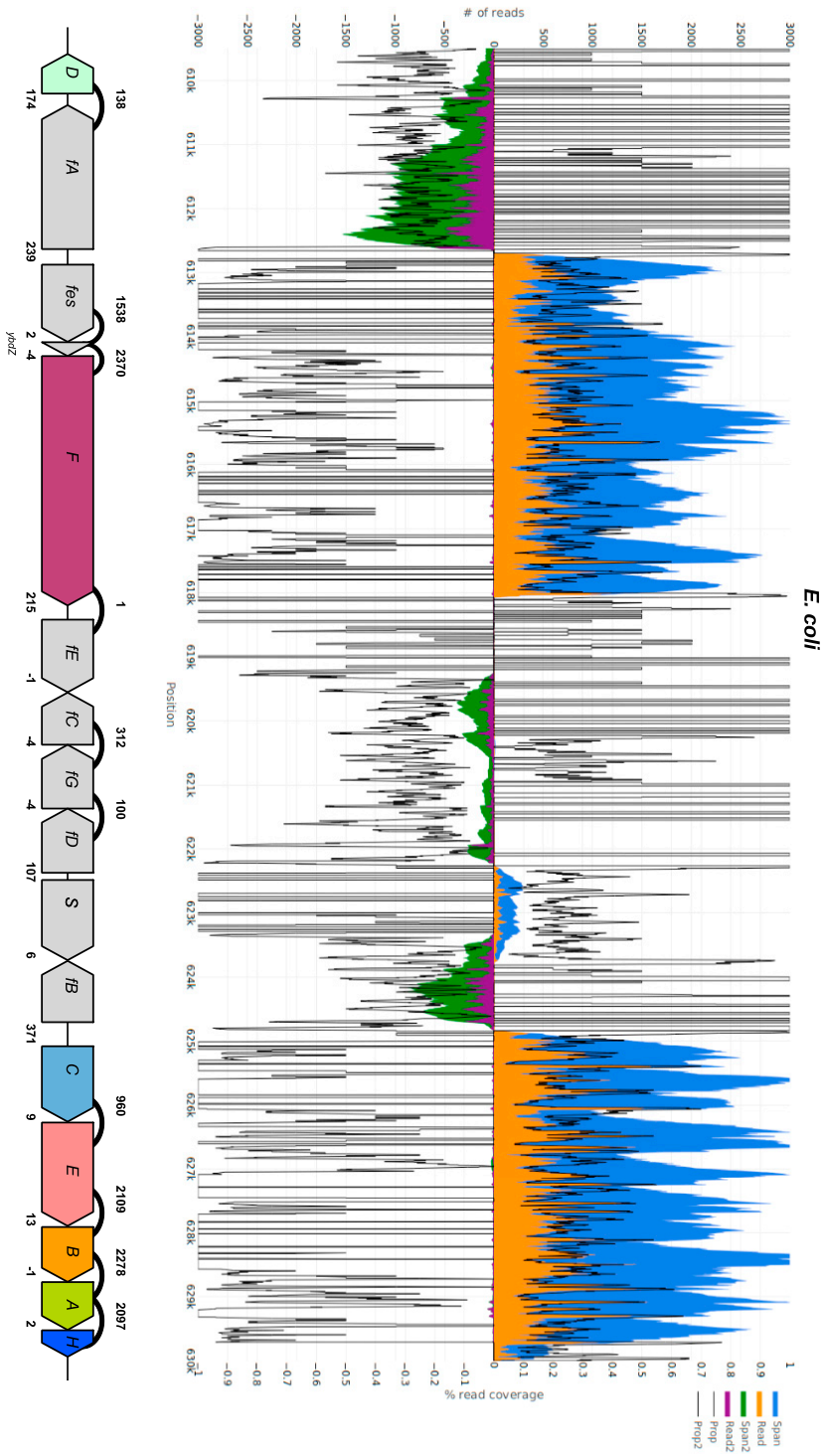

Figure S3. Transcriptomics of the Siderophore Biosynthesis Genes in *E. coli*, Related to Figure 4

(A) The orange area indicates per-base coverage by RNA-Seq reads (read coverage). The blue area indicates per-base cumulative coverage by RNA-Seq reads and inserts between read-pairs (span coverage). The purple area indicates read coverage of the opposite strand. The green area indicates span coverage of the opposite strand. The black lines indicate the ratios of the read coverage over the span coverage data for the relevant strand. (B) Diagram of siderophore biosynthesis genes as present in the *E. coli* genome drawn to scale. Counts above the diagram indicate read-pairs crossmapping between genes. Counts below indicate the size of intergenic regions between adjacent protein-coding sequences, in base pairs (negative numbers indicate overlap). The *f* prefix (*fA-fG*) indicates the *fepA-fepG* genes. All data based on Seo et al. (2014).

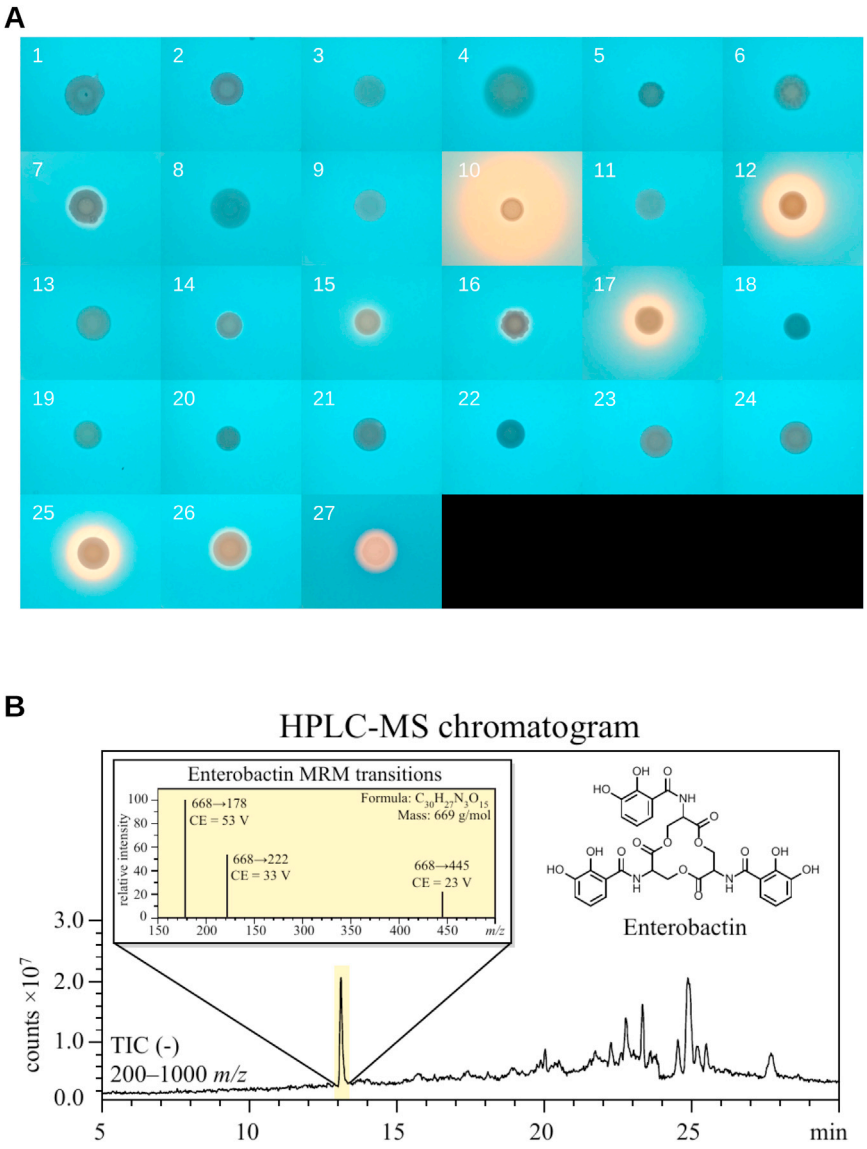

Figure S4. Detection of Enterobactin, Related to Figure 3

(A)O-CAS assay for all tested species. Species legend: (1) *Saccharomyces cerevisiae* FM1282 (negative control), (2) *Kluyveromyces lactis* CBS 2359, (3) *Tortispora caseinolytica* NRRL Y-17796^T, (4) *Yarrowia keelungensis* NRRL Y-63742^T, (5) *Yarrowia deformans* NRRL Y-321^T, (6) *Yarrowia lipolytica* NRRL YB-423^T, (7) *Blastobotrys adeninivorans* NRRL Y-17592, (8) *Sugiyamaella lignohabitans* NRRL YB-1473^T, (9) *Wickerhamiella hasegawae* JCM 12559^T, (10) *Wickerhamiella pararugosa* NRRL Y-17089^T, (11) *Wickerhamiella cacticola* NRRL Y-27362^T, (12) *Wickerhamiella versatilis* NRRL Y-6652^T, (13) *Starmerella gropengiesseri* NRRL Y-17142^T, (14) *Starmerella davenportii* CBS 9069^T, (15) *Starmerella ratchasimensis* CBS 10611^T, (16) *Starmerella apicola* NRRL Y-2481^T, (17) *Starmerella riodocensis* NRRL Y-27859^T, (18) *Wickerhamiella infanticola* NRRL Y-17858^T, (19) *Wickerhamiella occidentalis* NRRL Y-27364, (20) *Wickerhamiella domercqiae* NRRL Y-6692^T, (21) *Starmerella tilneyi* CBS 8794^T, (22) *Starmerella sorbosivorans* CBS 8768^T, (23) *Starmerella geochares* NRRL Y-17073^T, (24) *Starmerella vaccinii* NRRL Y-17684^T, (25) *Starmerella kuoi* NRRL Y-27208^T, (26) *Starmerella bombicola* NRRL Y-17069^T, and (27) *Escherichia coli* MG1655 (positive control). (B) Identification of enterobactin using HPLC-MS. Chromatogram shows a representative sample, from the culture of *Starmerella riodocensis.* The left insert shows the MS/MS fragmentation pattern used to confirm identity. The relative ratio of transitions was confirmed using authentic enterobactin standards. The right insert shows the biochemical structure of enterobactin.